E-ISSN: 2636-7688

february 2026
volume 33
issue 2

ANNALS OF MEDICAL RESEARCH

The Official Journal of the Inonu University Faculty of Medicine

Original Articles

İNÖNÜ UNIVERSITY PRESS

ANN MED RES

Ann Med Res

Annals of Medical Research

The Official Journal of Inonu University Faculty of Medicine

Editorial Board | Volume: 33 | Issue: 2 | February 2026

Ann Med Res

Annals of Medical Research

The Official Journal of Inonu University Faculty of Medicine

Editorial Advisory Board | Volume: 33 | Issue: 2 | February 2026

Ann Med Res

Annals of Medical Research

The Official Journal of Inonu University Faculty of Medicine

Table of Contents | Volume: 33 | Issue: 2 | February 2026

Original Articles

Ann Med Res

Current issue list available at Ann Med Res

Annals of Medical Research

journal page: annalsmedres.org

Evaluation of muscle strength and range of motion of upper extremity in breast cancer-related lymphedema

Furkan Kadir Gurlek [a], Hande Ozdemir [b],

[a] Trakya University, Health Sciences Institute, Edirne, Türkiye
[b] Trakya University, Faculty of Medicine, Department of Physical Medicine and Rehabilitation, Edirne, Türkiye
*Corresponding author: handeozdemirmd@gmail.com (Hande Ozdemir)

MAIN POINTS

- The study found that lymphedema after breast cancer treatment leads to a notable reduction in shoulder flexion and extension strength, as well as range of motion.
- Elbow flexion muscle strength was also significantly reduced in the affected arm.
- No significant differences were found in elbow extension, wrist flexion and extension strength, or the ROM of the elbow and wrist joints.
- The study's findings can assist clinicians in creating targeted rehabilitation programs that focus on restoring strength and mobility in the areas most impacted by lymphedema.

Cite this article as: Gurlek FK, Ozdemir H. Evaluation of muscle strength and range of motion of upper extremity in breast cancer-related lymphedema. *Ann Med Res*. 2026;33(2):48–55. doi: 10.5455/annalsmedres.2025.08.212.

ABSTRACT

Aim: The objective of this study was to examine the impact of lymphedema on the muscle strength and range of motion of the upper extremities in breast cancer patients with lymphedema.

Materials and Methods: Thirty-one female breast cancer survivors with lymphedema were evaluated in this cross-sectional study. The measurement of shoulder, elbow, and wrist flexion and extension strength was conducted using a hand-held dynamometer on both affected and unaffected upper extremities. Subsequently, a digital goniometer was utilized to assess the range of motion in both the affected and unaffected upper extremities.

Results: A median age of 61 years (with an interquartile range of 55 to 69 years) was reported for the patients, and dominant right upper extremity was noted for all. The study revealed that the affected extremity exhibited reduced shoulder flexion and extension muscle strength and range of motion, and decreased elbow flexion muscle strength when compared to the unaffected upper extremity ($p<0.05$). However, a lack of statistical significance was observed in the comparison of elbow extension, wrist flexion and extension strength, and elbow and wrist joint range of motion between the two extremities ($p>0.05$).

Conclusion: In cancer-associated lymphedema, limitations in muscle strength and range of motion are primarily localized to the shoulder region. These findings may serve as a guide for clinicians in the development of targeted rehabilitation interventions, with the aim of restoring mobility and strength in the areas most affected by lymphedema.

Keywords: Lymphedema, Muscle strength, Range of motion

Received: Aug 06, 2025 **Accepted:** Oct 02, 2025 **Available Online:** Feb 25, 2026

INTRODUCTION

A significant increase in the burden of breast cancer has been detected in middle- and low-income countries, particularly over the last three decades, due to differences in access to health resources [1]. About 20% of patients with breast cancer develop lymphedema, which can be caused by obstruction or disruption in the lymphatic system resulting from cancer treatment [2]. Lymphedema causes swelling of an extremity due to excessive accumulation of a protein-rich fluid [3]. Symptoms include pain, a sense of heaviness, and impaired motor abilities, daily functioning, and quality of life [4,5]. Women undergoing breast cancer treatment are prone to developing upper extremity muscle weakness and range of motion (ROM) limitations, even in the absence of lymphedema [6,7]. These impairments are underpinned by physiological factors such as nerve damage from surgery, fibrotic tissue formation from radiation therapy, and muscle ischemia, as well as behavioral factors such as kinesiophobia, where patients avoid using the affected arm out of fear of worsening lymphedema [8-11].

The majority of studies that have focused on upper extremity function in cases of breast cancer-related lymphedema have concentrated on the measurement of shoulder girth or the assessment of hand grip strength. However, existing literature

is either contradictory or deficient in its specific discussion of changes in muscle strength and range of motion (ROM) in more distal joints, including the elbow and wrist. For instance, some studies have identified a correlation between weakness in grip strength and lymphedematous extremities [12], while others have found no significant difference in hand grip strength or dexterity between affected and unaffected sides in lymphedema patients [13,14]. This finding indicates that the functionality of distal joints may be partially preserved, irrespective of the presence of lymphedema or through patients' adaptations to daily activities.

Given these variability in the existing literature and the lack of objective assessments focusing on specific joints, it is crucial to comprehensively examine flexion and extension muscle strength and ROM in the shoulder, elbow, and wrist joints in patients with breast cancer-associated lymphedema. By comparing these parameters between lymphedematous and non-lymphedematous arms, this study aims to further elucidate the specific effects of lymphedema on different regions of the upper extremity, thereby contributing scientifically to the development of rehabilitation strategies.

MATERIALS AND METHODS

Study design

This cross-sectional study was conducted in Trakya University Faculty of Medicine, Physical Therapy and Rehabilitation Outpatient Clinic Lymphedema Unit between September 2021 and September 2022 with the approval of Trakya University Faculty of Medicine Scientific Research Ethics Committee dated 14.06.2021 with protocol number TÜTF-BAEK 2021/277 and designed in compliance with the 2008 Declaration of Helsinki. All participants in the study have provided written consent.

Participants

The sample size of the study was determined as 34 patients, using an effect size of 0.496, an error rate of 5%, and a power value of 80%, based on the hand grip strength values of lymphedema patients in the study conducted by Erdoğanoğlu et al. [15]. However, only 33 patients were evaluated for eligibility. Women aged 18-75 years with unilateral upper extremity lymphedema associated with breast cancer were included. Patients had to have completed radiotherapy and chemotherapy for breast cancer at least 6 weeks prior and surgical treatment at least 3 months prior. Exclusion criteria were bilateral breast cancer or lymphedema, metastatic or recurrent breast cancer, acute upper extremity infection, or neuromusculoskeletal disease affecting upper extremity tests. After excluding two patients who failed to meet the specified inclusion criteria, the study sample comprised a total of 31 patients.

Assessments

Patients diagnosed with unilateral upper extremity lymphedema were asked to provide information regarding their age, height, body weight, marital status, educational level, and employment status. The body mass index (BMI) was computed as the weight (kg) divided by the height (m) squared. Weight categories : underweight (BMI < 18.5); normal (18.5–24.99); overweight (25–29.99); class 1 obesity (30–34.99); class 2 obesity (35–39.99); and class 3 obesity (40 and above) [16]. Patients were queried about their receipt of chemotherapy and/or radiotherapy. The Visual Analog Scale (VAS) was used to evaluate the average degree of pain in the affected arm over the past week [17]. The International Physical Activity Questionnaire (Short Form) was given to assess physical activity levels [18]. The Edinburgh hand preference questionnaire was used to determine the dominant upper extremities [19]. Upper extremity circumference, muscle strength, and range of motion measurements were performed using validated and reliable methods by a single evaluator [20-22]. The measurement of the patient's upper limb circumference was taken in a supine position with both arms at their sides, using a tape measure. The measurements were obtained at the level of the first and fifth metacarpophalangeal joints, followed by the measurement of 4-centimeter intervals along the limb, commencing at the ulnar styloid process [20]. The lymphedema staging was carried out based on the International Society of Lymphology (ISL) staging system [23]. Muscle strength was assessed in the subjects using a hand-held dynamometer (HHD) (Lafayette Instrument, USA). They were asked to take standard positions and apply resistance against the dynamometer. They were given a trial application, then instructed to reach maximum contraction with the initial warning signal and maintain it until the subsequent signal. The measurement was repeated after a one-minute interval, and the higher value was documented. The strength of the muscles on both sides of the body was measured with the patient lying supine on a stretcher. The HHD was positioned posterior to the forearm, with the shoulder in 90° flexion, the elbow and wrist in a neutral position, and the forearm in pronation to assess the strength of the shoulder flexor muscles. The HHD was positioned anterior to the forearm, with the shoulder in 90° flexion, the elbow and wrist in a neutral position, the forearm pronated to assess the strength of the shoulder extensor muscles. To evaluate the strength of the elbow flexor muscles, the HHD was placed on the anterior aspect of the forearm, with the shoulder and wrist at 0°, elbow in 90° flexion, and forearm supinated. To measure the strength of the elbow extensor muscles, the HHD was placed posterior to the forearm, with the shoulder and wrist at 0°, elbow at 90° flexion, forearm supinated. To evaluate the strength of the wrist flexor muscles, the HHD was placed anterior to the carpal surface, with the shoulder in 30° abduction, the elbow and wrist in 0°, the forearm supinated, the wrist outside the stretcher. To measure the strength of the wrist extensor muscles, the HHD was placed posterior to the carpal surface, with the shoulder in 30° abduction, the elbow and wrist in 0° flexion, the forearm in pronation, the wrist extending beyond

https://doi.org/10.5455/annalsmedres.2025.08.212

the stretcher (Figure 1) [21, 24, 25]. The digital goniometer (Baseline Absolute+ Axis, Newyork,USA) was utilized to determine the ROMs of shoulder flexion, shoulder extension, elbow flexion, elbow extension, and wrist flexion and wrist extension of both upper extremities [22, 26].

Sensitivity analysis

To evaluate the robustness of the findings given the modest shortfall in sample size (31 instead of 34 patients), a leave-one-out sensitivity analysis was performed for all paired outcomes. Each Wilcoxon signed-rank test was repeated after sequentially excluding one participant at a time, and the resulting range of p-values was recorded.

Statistical analysis

The study's data were processed using Statistical Software Package for Social Sciences (SPSS) for Windows, version 20.0 (license number 10240642). Continuous variables were expressed as mean ± standard deviation and median (IQR 25-75), while categorical variables were expressed as number and percentage. In statistical evaluations, the conformity of the data to normal distribution was evaluated by one sample Kolmogorov Smirnov test. Wilcoxon signed rank test was used to compare affected and unaffected upper extremity muscle strength and ROMs of the participants. Any $p<0.05$ was considered as statistical significance.

RESULTS

This study included 31 female patients, aged 55 to 69, with unilateral upper extremity lymphedema. Among these participants, 77% were overweight or obese, and 93% were minimally active or physically inactive. The dominant arm for all patients was the right, while the lymphedema-affected extremity was the non-dominant arm in 71% of cases. The majority of patients presented with stage 1 lymphedema, followed by stage 2 and stage 3. Patient demographics and clinical characteristics are detailed in Table 1.

A comparison of muscle strength between the affected and unaffected upper extremities revealed statistically significant deficits in the affected arm for shoulder flexion, shoulder extension, and elbow flexion (Table 2). Sensitivity analyses confirmed the robustness of these findings; leave-one-out p-value ranges remained below 0.05 for shoulder flexion (<.001–.002), shoulder extension (.009–.051), and elbow flexion (.005–.031). No significant differences were observed for elbow extension or wrist flexion and extension, and sensitivity analyses confirmed the stability of these null results.

The range of motion of the affected and unaffected extremities is compared in Table 3. Shoulder flexion and extension were significantly reduced on the affected side ($p = .008$ and $p = .035$, respectively). Sensitivity analyses confirmed these findings were robust (p-value ranges of .001–.013 and .009–.059, respectively). No significant differences were observed for elbow or wrist ROMs, and these null findings were again supported by the sensitivity results.

DISCUSSION

Among individuals with unilateral lymphedema following breast surgery, this study identified decreased muscle strength in shoulder flexion, shoulder extension, and elbow flexion, as well as reduced ROM in shoulder flexion and extension in the affected extremity compared to the unaffected one. However, no significant differences were found in elbow extension strength, wrist flexion/extension strength, or elbow and wrist joint ROMs between the two extremities. These findings are consistent with some reports in the literature but contradict others.

Arm weakness is a commonly reported complication, affecting 23-28% of patients after breast surgery [27, 28]. It is well-established that women undergoing treatment for breast cancer are susceptible to developing muscle weakness and impaired mobility, even without lymphedema [6, 7]. In a 5-year follow-up, Belmonte et al. [7] found that breast cancer patients who underwent axillary lymph node dissection—a procedure associated with a higher lymphedema incidence than sentinel lymph node biopsy—experienced significant strength loss in the internal rotators of the affected shoulder. This muscle weakness can be attributed to several factors, including nerve damage during axillary dissection, radiation-induced fibrosis, and sensory impairment [8-10]. Furthermore, scapular rhythm disturbances and the overworking of compensatory muscles can negatively affect muscle strength and endurance [9]. Consistent with our findings, previous studies have also noted decreased strength in shoulder abduction, adduction, external rotation, and trapezius muscles [6], as well as in shoulder internal and external rotation [9], in women with lymphedema.

A notable finding from our study, which aligns with existing literature, is the decreased elbow flexor strength in the lymphedematous limb. Smoot et al. [14] similarly reported reduced elbow flexor strength on the affected side in women with lymphedema, who also experienced significant difficulty carrying objects heavier than 4.5 kg. These findings suggest that lymphedema is not merely a volumetric issue but one that directly impairs upper extremity muscle function. The development of muscle strength deficits after breast surgery is multifactorial and not solely determined by lymphedema volume. Lee et al. [11] proposed that weakness in the affected arm may not be a direct result of the disease itself but rather from a reluctance to use the arm due to a fear of movement, a phenomenon known as kinesiophobia. This fear can trigger "use-avoidance" behaviors, leading to muscle atrophy and functional decline. Therefore, all patients with lymphedema post-breast surgery should undergo a comprehensive evaluation of upper extremity muscle strength and function. Multidisciplinary interventions, including specialized rehabilitation with resistance exercises, are crucial for managing the condition and have been shown to improve functional capacity and quality of life [29].

In contrast to some reports, our finding that wrist flexion and

https://doi.org/10.5455/annalsmedres.2025.08.212

Table 1. Demographic and clinical characteristics of the patients.

Variables		All cases (n=31)
Age, years	Mean (SD) Median (IQR)	60.81 (9.46) 61 (55-69)
Height, cm	Mean (SD) Median (IQR)	158.06 (4.75) 156 (155-161)
Body weight, kg	Mean (SD) Median (IQR)	79 (17.15) 79 (67-88)
BMI, kg/m²	Mean (SD) Median (IQR)	31.70 (7.31) 31.25 (25.20-35.15)
Weight status category	n (%)	
Underweight		0
Normal		7 (22.6)
Overweight		6 (19.4)
Class 1 obesity		10 (32.3)
Class 2 obesity		4 (12.9)
Class 3 obesity		4 (12.9)
Marital status	n (%)	
Married		27 (87.1)
Single		1 (3.2)
Widowed		3 (9.7)
Educational Level	n (%)	
Illiterate		1 (3.2)
Primary School		15 (48.4)
Middle School		6 (19.4)
High School		6 (19.4)
Undergraduate		3 (9.7)
Employment Status	n (%)	
Housewife		23 (74.2)
Retired		5 (16.1)
Employed		3 (9.7)
History of receiving chemotherapy and/or radiotherapy	n (%)	
None		1 (3)
Chemotherapy		4 (13)
Chemotherapy and radiotherapy		26 (84)
VAS (1-10)	Mean (SD) Median (IQR)	2.45 (3.02) 1 (0-4)
Physical activity level (MET-min/week)	Mean (SD) Median (IQR)	1349.27 (1995.35) 693 (396-1386)
Physical activity category	n (%)	
Low		12 (38.7)
Moderate		17 (54.8)
High		2 (6.5)
Distribution of lymphedema according to upper extremity dominance	n (%)	
Lymphedema in the dominant upper extremity		9 (29)
Lymphedema in the non-dominant upper extremity		22 (71)
Lymphedema Stage	n (%)	
Stage 1		12 (38.7)
Stage 2		11 (35.5)
Stage 3		8 (25.8)

BMI: body mass index , MET: metabolic equivalent of task, VAS: visual analogue scale.

extension strength in the lymphedematous extremity was similar to the unaffected side offers a more nuanced view of upper extremity weakness. Smoot et al. [14] found a decline in wrist flexion strength in the affected arm, and Baklacı et al. [12] demonstrated that hand grip strength was diminished in the lymphedematous arm, even after complete decongestive therapy. However, the latter study also noted that changes in hand grip strength can occur regardless of surgery type or the presence of lymphedema [12]. Supporting our results, a study by Civelek [13] revealed no statistically significant difference in hand grip strength or function between the affected and unaffected sides of patients with lymphedema. This sug-

https://doi.org/10.5455/annalsmedres.2025.08.212

Table 2. Comparison of affected and unaffected upper extremity flexion and extension muscle strengths.

Muscle strength (kg)	Affected upper extremity Mean (SD) Median (IQR) (n=31)	Unaffected upper extremity Mean (SD) Median (IQR) (n=31)	p*	Sensitivity p-value (LOO range)**
Shoulder flexion	7.16 (2.18) 7.20 (5.4-8.9)	8.29 (1.83) 8.4 (7.2-9.2)	.002	<.001-.002
Shoulder extension	7.93 (2.05) 8.3 (7.3-8.8)	8.72 (1.72) 8.4 (8.0-9.9)	.028	.009-.051
Elbow flexion	12.57 (3.67) 13.10 (9.8-15.1)	13.77 (2.91) 13.3 (11.7-15.5)	.018	.005-.031
Elbow extension	10.09 (2.71) 10 (8.8-11.4)	10.89 (2.25) 10.9 (9.6-12.3)	.225	.137-.336
Wrist flexion	6.64 (2.07) 6.0 (5.1-8.0)	6.87 (1.77) 6.4 (5.6-7.8)	.239	.124-.349
Wrist extension	7.68 (2.36) 7.7 (5.6-9.6)	7.26 (1.87) 7.2 (5.8-8.2)	.156	.076-.256

*p value by Wilcoxon Signed Ranks Test. Statistically significant p–value < 0.05. ** Sensitivity p-values indicate the range observed in leave-one-out analysis.

Table 3. Comparison of affected and unaffected upper extremity range of motions.

Range of motion (°)	Affected upper extremity Mean (SD) Median (IQR) (n=31)	Unaffected upper extremity Mean (SD) Median (IQR) (n=31)	p*	Sensitivity p-value (LOO range)**
Shoulder flexion	144.61 (24.51) 146 (130-160)	156.10 (22.02) 160 (150-170)	.008	.001 -- .013
Shoulder extension	56.26 (12.24) 55 (49-67)	60.19 (11.18) 60 (50-70)	.035	.009 -- .059
Elbow flexion	132.23 (9.71) 135 (130-140)	135.10 (8.32) 135 (130-140)	.267	.188 -- .439
Elbow extension	1.06 (2.59) 0 (0-3)	-0.35 (4.05) 0 (0-0)	.068	.027 -- .151
Wrist flexion	67.61 (9.15) 65 (60-75)	67.93 (10.47) 69 (62-75)	.909	.665 -- 1.000
Wrist extension	64.71 (12.36) 63 (60-75)	61.39 (12.36) 65 (54-70)	.243	.144 -- .386

*p value by Wilcoxon Signed Ranks Test. Statistically significant p–value < 0.05. **Sensitivity p-values indicate the range observed in leave-one-out analysis.

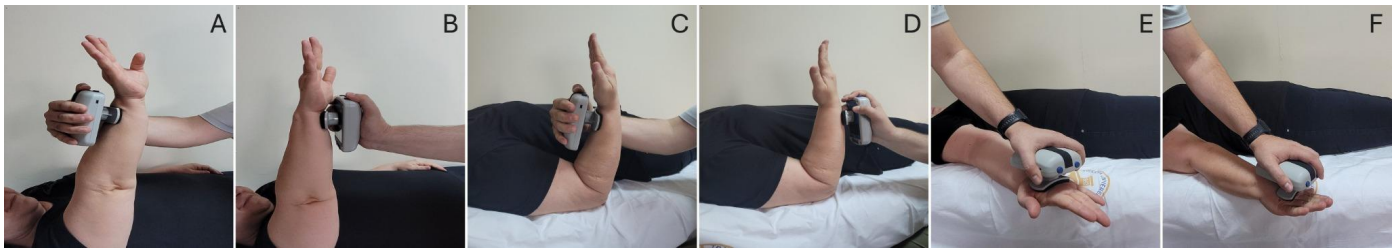

Figure 1. Isometric strength testing positions using the handheld dynamometer. (A) shoulder flexion, (B) shoulder extension, (C) elbow flexion, (D) elbow extension, (E) wrist flexion, (F) wrist extension.

gests that while surgical and therapeutic interventions impact overall upper extremity function, the adaptive capacity of distal joints like the wrist may mask these deficits. Patients may maintain fine motor skills in their hands and wrists for daily activities despite the severity of or apprehension about their lymphedema [13]. Additionally, kinesiophobia may primarily limit proximal movements at the shoulder and elbow, while less-feared movements of the wrist remain relatively unaffected.

Our observation of limited shoulder flexion and extension

https://doi.org/10.5455/annalsmedres.2025.08.212

in the affected extremity is consistent with the literature. Postoperative shoulder limitations are documented in 28.3% of patients after breast surgery and are correlated with increased upper extremity disability [14, 27]. Lymphedema can exacerbate these limitations. Rezende et al. [6] observed that women who underwent mastectomy had more restricted shoulder flexion, abduction, and rotation ROMs on the affected side, with limitations being more pronounced in those with lymphedema. These shoulder limitations can be attributed to factors such as scar tissue formation, radiation-induced fibrosis, protective posturing, and prolonged immobility or pain [14]. Our findings on distal joint ROM, however, reveal some discrepancies with previous research. The similar elbow ROM we observed between extremities is consistent with Smoot et al. [14]. Yet, while they noted a greater limitation in wrist flexion on the affected side, our study found comparable wrist ROM in both arms. This discrepancy may be due to differences in patient populations. In the study by Smoot et al., 52% of patients had lymphedema in their dominant extremity, whereas this figure was only 29% in our study. It is plausible that when the dominant hand is affected, patients may use it less out of concern for worsening symptoms, leading to reduced strength and mobility. Since the majority of our patients had lymphedema in the non-dominant limb, this effect may not have been present. However, this explanation should be interpreted cautiously, as Smoot et al. [14] found that limb dominance did not significantly affect functional disability scores. Methodological differences, such as goniometer sensitivity, measurement techniques, or sample size, could also contribute to these divergent results [14].

In our cohort, the affected extremity was the non-dominant (left) arm in 71% of patients, which aligns with the higher incidence of left-sided breast cancer in the general population [30]. This suggests that the prevalence of lymphedema may mirror the anatomical distribution of breast cancer. This finding is clinically significant, as some data indicate that left-sided breast cancers may have a more aggressive biological profile and less favorable long-term outcomes [31]. The literature is conflicting regarding the relationship between the treated side's dominance and lymphedema risk. Hayes et al. [32] reported an 80% higher risk of lymphedema in patients treated on the non-dominant side, suggesting that greater use of the dominant arm in daily life may be protective. Conversely, Bulley et al. [33] found no association between limb dominance and the development of lymphedema or upper extremity dysfunction. Future research should investigate the complex interplay between lymphedema localization, surgical factors, and long-term patient outcomes.

Limitations

This study has several limitations. First, its cross-sectional design precludes the establishment of causal relationships. Nonetheless, the data provide clinicians with valuable observational findings to guide patient evaluations. Second, the final sample size of 31 patients was slightly below our target of 34. Although a sensitivity analysis was performed to assess the robustness of the findings, the reduced sample size may still limit generalizability. Third, the absence of a healthy control group makes it difficult to ascertain whether the observed impairments are solely attributable to lymphedema or are influenced by confounding factors such as age-related decline. However, the within-subject comparison design is a strength, as it minimizes the impact of inter-individual factors like general health and lifestyle. Finally, due to a lack of data, we could not assess clinical parameters such as the specific type of malignancy, whether axillary dissection was performed, or the surgical procedure used. This prevented an analysis of how different treatments might affect upper extremity outcomes. Future longitudinal studies with more comprehensive data collection are needed to elucidate causal relationships and refine clinical practice.

CONCLUSION

In conclusion, this study demonstrates that patients with upper extremity lymphedema following breast cancer treatment have significant deficits in shoulder flexion/extension (both strength and ROM) and elbow flexion strength in the affected limb. These impairments appear to be localized to the proximal joints, which provides a clear rationale for targeted rehabilitation. Treatment programs should focus on addressing the pronounced limitations around the shoulder while leveraging the preserved function of the elbow and wrist. This targeted approach allows clinicians to prioritize interventions to restore mobility and strength where it is most needed.

Data Availability Statement: The underlying data presented in this publication are available upon reasonable request to the corresponding author.

Ethics Committee Approval: The study was approved by the Trakya University Scientific Research Ethics Committee (Decision No: TÜTF-BAEK:2021/277 Date: 14.06.2021).

Informed Consent: The authors stated that they obtained informed consent from the participants in the study.

Peer-review: Externally peer-reviewed.

Conflict of Interest: The authors declared that they have no conflict of interest.

Author Contributions: Conception: FKG, HO; Design: FKG, HO; Supervision: FKG, HO; Materials: FKG, HO; Data collection and proccessing: FKG, HO; Analysis and interpretion: FKG, HO; Literature review: FKG, HO; Writing and critical review: FKG, HO.

Financial Disclosure: The authors received no financial support for the research, authorship, and/or publication of this article.

https://doi.org/10.5455/annalsmedres.2025.08.212

Artificial Intelligence Disclosure: During the preparation of this manuscript, the authors used DeepL (DeepL SE, Cologne, Germany) to improve the language and readability of the text. After using this tool, the authors reviewed and edited the content as needed and take full responsibility for the accuracy and integrity of the final version of the manuscript.

REFERENCES

1. Cai Y, Dai F, Ye Y, Qian J. The global burden of breast cancer among women of reproductive age: a comprehensive analysis. *Sci Rep*. 2025;15(1):9347. doi: 10.1038/s41598-025-93883-9.
2. DiSipio T, Rye S, Newman B, Hayes S. Incidence of unilateral arm lymphoedema after breast cancer: a systematic review and meta-analysis. *Lancet Oncol*. 2013;14(6):500-15. doi: 10.1016/S1470-2045(13)70076-7.
3. Cheville AL, McGarvey CL, Petrek JA, Russo SA, Thiadens SR, Taylor ME. The grading of lymphedema in oncology clinical trials. *Semin Radiat Oncol*. 2003: 13(3):214-25. doi:10.1016/S1053-4296(03)00038-9.
4. Hayes SC, Johansson K, Stout NL, Prosnitz R, Armer JM, Gabram S, et al. Upper-body morbidity after breast cancer: incidence and evidence for evaluation, prevention, and management within a prospective surveillance model of care. *Cancer*. 2012;118(S8):2237-49. doi: 10.1002/cncr.27467.
5. Shaitelman SF, Cromwell KD, Rasmussen JC, Stout NL, Armer JM, Lasinski BB, et al. Recent progress in the treatment and prevention of cancer-related lymphedema. *CA Cancer J Clin*. 2015;65(1):55-81. doi: 10.3322/caac.21253.
6. Rezende MS, Rossi DM, de Lima AMR, Clemente GS, de Oliveira AS, de Oliveira Guirro EC. Shoulder and scapulothoracic impairments in women with breast cancer-related lymphedema in the upper limb: a cross-sectional study shoulder and breast cancer-related lymphedema. *J Bodyw Mov Ther*. 2024;37:177-82. doi: 10.1016/j.jbmt.2023.11.055.
7. Belmonte R, Messaggi-Sartor M, Ferrer M, Pont A, Escalada F. Prospective study of shoulder strength, shoulder range of motion, and lymphedema in breast cancer patients from pre-surgery to 5 years after ALND or SLNB. *Support Care Cancer*. 2018;26(9):3277-87. doi: 10.1007/s00520-018-4186-1.
8. Lebel S, Tomei C, Feldstain A, Beattie S, McCallum M. Does fear of cancer recurrence predict cancer survivors' health care use? *Support Care Cancer*. 2013;21(3):901-6. doi: 10.1007/s00520-012-1685-3.
9. Zabit F, Iyigun G, Malkoc M. Assessment of proprioception, muscle strength and endurance during dynamic isokinetic test in patients with breast cancer-related lymphedema. *Clin Biomech*. 2023;110:106100. doi: 10.1016/j.clinbiomech.2023.106100.
10. Belmonte R, Monleon S, Bofill N, Alvarado ML, Espadaler J, Royo I. Long thoracic nerve injury in breast cancer patients treated with axillary lymph node dissection. *Support Care Cancer*. 2015;23(1):169-75. doi: 10.1007/s00520-014-2338-5.
11. Lee D, Hwang JH, Chu I, Chang HJ, Shim YH, Kim JH. Analysis of factors related to arm weakness in patients with breast cancer-related lymphedema. *Support Care Cancer*. 2015;23(8):2297-304. doi: 10.1007/s00520-014-2584-6.
12. Baklaci M, Eyigör S, Tanıgör G, Özgür İnbat M, Çalışkan Kabayel S. Assessment of muscle strength and volume changes in patients with breast cancer-related lymphedema. *Oncol Res Treat*. 2020;43(11):584-91. doi: 10.1159/000509672.
13. Civelek GM. Effects of breast cancer related lymphedema on hand muscle strength, hand functions and sensory loss of hand. *Cukurova Med J*. 2016;41(2):208-16. doi: 10.17826/cutf.200040.
14. Smoot B, Wong J, Cooper B, Wanek L, Topp K, Byl N, et al. Upper extremity impairments in women with or without lymphedema following breast cancer treatment. *J Cancer Surviv*. 2010;4(2):167-78. doi: 10.1007/s11764-010-0118-x.
15. Erdoğanoğlu Y, Çalık M, Vural M. Functional evaluation of patients with mastectomy lymphedema. *Turk J Phys Med Rehabil*. 2021;67(1):56. doi: 10.5606/tftrd.2021.4616.
16. Douketis JD, Paradis G, Keller H, Martineau C. Canadian guidelines for body weight classification in adults: application in clinical practice to screen for overweight and obesity and to assess disease risk. *CMAJ*. 2005;172(8):995-8. doi: 10.1503/cmaj.045170.
17. Kahl C, Cleland JA. Visual analogue scale, numeric pain rating scale and the McGill pain Questionnaire: an overview of psychometric properties. *Physical Therapy Reviews*. 2005;10(2):123-8. doi: 10.1179/108331905X55776.
18. Saglam M, Arikan H, Savci S, Inal-Ince D, Bosnak-Guclu M, Karabulut E, et al. International physical activity questionnaire: reliability and validity of the Turkish version. *Percept Mot Skills*. 2010;111(1):278-84. doi: 10.2466/06.08.PMS.111.4.278-284.
19. Uysal SA, Ekinci Y, Çoban F, Yakut Y. Edinburgh el tercihi anketi Türkçe güvenirliğinin araştırılması. *JETR*. 2019;6(2):112-8.
20. Meijer RS, Rietman JS, Geertzen JH, Bosmans JC, Dijkstra PU. Validity and intra- and interobserver reliability of an indirect volume measurements in patients with upper extremity lymphedema. *Lymphology*. 2004;37(3):127-33. PMID: 15560108.
21. Rheault W, Beal JL, Kubik KR, Nowak TA, Shepley JA. Intertester reliability of the hand-held dynamometer for wrist flexion and extension. *Arch Phys Med Rehabil*. 1989;70(13):907-10. PMID: 2596965.
22. Carey MA, Laird DE, Murray KA, Stevenson JR. Reliability, validity, and clinical usability of a digital goniometer. *Work*. 2010;36(1):55-66. doi: 10.3233/WOR-2010-1007.
23. Executive Committee of the International Society of Lymphology. The Diagnosis and Treatment of Peripheral Lymphedema: 2016 Consensus Document of the International Society of Lymphology. *Lymphology*. 2016;49(4):170-84. PMID: 29908550.
24. Nepomuceno Júnior BRV, Menezes MPdS, Santos KRBd, Gomes Neto M. Comparison of methods for evaluating upper limb strength by hand-held dynamometry. *Rev Bras Med Esporte*. 2021;27:42-8. doi: 10.1590/1517-8692202127012020_0008.
25. Douma RK, Soer R, Krijnen WP, Reneman M, Van Der Schans CP. Reference values for isometric muscle force among workers for the Netherlands: a comparison of reference values. *BMC Sports Sci Med Rehabil*. 2014;6(1):10. doi: 10.1186/2052-1847-6-10.
26. Norkin CC, White DJ. Measurement of joint motion: a guide to goniometry. 5th ed. Philadelphia: *FA Davis*; 2016.
27. Mollaoglu MC, Mollaoğlu M, Akın EB, Karadayı K. Meme Kanseri Cerrahisi Sonrası Üst Ekstremite Sorunları ve Yeti Yitimi. *IGUSAB-DER*. 2024(23):750-66.
28. Lee TS, Kilbreath SL, Refshauge KM, Herbert RD, Beith JM. Prognosis of the upper limb following surgery and radiation for breast cancer. *Breast Cancer Res Treat*. 2008;110(1):19-37. doi: 10.1007/s10549-007-9710-9.
29. Lin Y, Wu C, He C, Yan J, Chen Y, Gao L, et al. Effectiveness of three exercise programs and intensive follow-up in improving quality of life, pain, and lymphedema among breast cancer survivors: a randomized, controlled 6-month trial. *Support Care Cancer*. 2023;31(1):9. doi: 10.1007/s00520-022-07494-5.
30. Badru F, Chianakwalam C, Stevenson V. Laterality of Breast Cancer-is it true? *Eur J Surg Oncol*. 2011;37(11):987. doi: 10.1016/j.ejso.2011.08.044.
31. Abdou Y, Gupta M, Asaoka M, Attwood K, Mateusz O, Gandhi S, et al. Left sided breast cancer is associated with aggressive biology and worse outcomes than right sided breast cancer. *Sci Rep*. 2022;12(1):13377. doi: 10.1038/s41598-022-16749-4.
32. Hayes S, Cornish B, Newman B. Comparison of methods to diagnose lymphoedema among breast cancer survivors: 6-month follow-up. *Breast Cancer Res Treat*. 2005;89(3):221-6. doi: 10.1007/s10549-004-2045-x.

https://doi.org/10.5455/annalsmedres.2025.08.212

33. Bulley C, Coutts F, Blyth C, Jack W, Chetty U, Barber M, et al. Prevalence and impacts of upper limb morbidity after treatment for breast cancer: a cross-sectional study of lymphedema and function. *Cancer and Oncology Research.* 2013;1(2):30-39. doi: 10.13189/cor.2013.010203.

https://doi.org/10.5455/annalsmedres.2025.08.212

Ann Med Res

Current issue list available at Ann Med Res

Annals of Medical Research

journal page: annalsmedres.org

Renal outcomes of children with ectopic kidneys: A single-center experience

Zehra Aydin [a],*, Emine Ozlem Cam Delebe [a]

[a] *Gaziantep City Hospital, Clinic of Pediatric Nephrology, Gaziantep, Türkiye*
**Corresponding author: mdzehraydn@gmail.com (Zehra Aydin)*

MAIN POINTS

- Renal ectopia was frequently associated with left-sided involvement in this pediatric cohort.
- Crossed renal ectopia (CRE) was observed in 15.5% of the patients, with 77.7% showing crossed-fused anatomy.
- Additional urogenital anomalies, including hydronephrosis, neurogenic bladder, vesicoureteral reflux, and duplicated collecting systems, were common.
- Renal scarring was detected in 8 patients, all with vesicoureteral reflux, emphasizing the need for early detection and follow-up.
- Consanguinity and positive family history of CAKUT were frequent, highlighting potential genetic predisposition in renal ectopia.

Cite this article as: Aydin Z, Cam Delebe EO. Renal outcomes of children with ectopic kidneys: A single-center experience. *Ann Med Res*. 2026;33(2):56–59. doi: 10.5455/annalsmedres.2025.08.226.

ABSTRACT

Aim: This study aimed to evaluate the clinical characteristics, associated anomalies, and outcomes of children diagnosed with renal ectopia in a single tertiary care center.

Materials and Methods: We retrospectively reviewed the medical records of 58 children with renal ectopia who were followed up between January 2024 and June 2025. Data on demographics, anomalies, laboratory findings, imaging findings, and treatments were analyzed.

Results: Among 58 patients (mean age 71.6 ± 56.4 months; 33 females, 25 males), 26 (44.8%) had right renal ectopia and 32 (55.2%) had left renal ectopia. Crossed renal ectopia was present in 9 (15.5%) patients, of whom 7 (77.8%) had crossed-fused renal ectopia. Additional urogenital anomalies included hydronephrosis in 7 (12.1%), neurogenic bladder in 4 (6.9%), and vesicoureteral reflux in 3 (5.2%). Prenatal diagnosis was achieved in 4 (6.9%) patients. Consanguinity was noted in 28 patients (48.3%), and 11 patients (19.0%) had a family history of CAKUT. Voiding cystourethrography was performed in 12 patients (20.7%) and high-grade vesicoureteral reflux was identified in 3 patients. Renal scarring was detected in 8 (15.1%) of the 53 patients who underwent DMSA scintigraphy; of these, 1 patient had hypertension, 1 had proteinuria, 1 was followed with stage 2 chronic kidney disease, and 1 with stage 5 chronic kidney disease.

Conclusion: Renal ectopia may be accompanied by additional urogenital anomalies. Early diagnosis and comprehensive evaluation are essential for optimal management and prognosis.

Keywords: Renal ectopia, Crossed renal ectopia, Congenital anomalies

Received: Aug 18, 2025 **Accepted:** Oct 23, 2025 **Available Online:** Feb 25, 2026

INTRODUCTION

Renal ectopia refers to the abnormal positioning of one or both kidneys due to disrupted renal ascent during fetal development. It occurs in approximately 1 in 900 live births and is more frequently observed in males [1]. Ectopic kidneys may be located in various anatomical regions, including the pelvic, iliac, abdominal, or, more rarely, thoracic areas [2].

Renal ectopia is classified as either simple ectopia—where the kidney is located on the correct side but in an abnormal position—or crossed ectopia, in which the kidney crosses to the opposite side. The ectopic kidney is fused with the contralateral kidney in most cases of crossed renal ectopia (approximately 90%), a condition known as crossed-fused renal ectopia [3]. Crossed-fused renal ectopia is identified in approximately 1 in 7500 autopsies, whereas nonfused crossed renal ectopia is considerably rarer, occurring in approximately 1 in 75,000 cases [4].

Although many children with renal ectopia are asymptomatic, the condition may lead to various urological complications. These include ureteral obstruction, recurrent urinary tract infections, and urolithiasis. Hydronephrosis (56%), vesicoureteral reflux (30%), and ureteropelvic junction obstruction (29%) are among the most common complications. Affected kidneys may develop cystic dysplasia, calculi, or malignancies less frequently [2,3].

Renal ectopia is also frequently associated with other congenital anomalies, particularly crossed ectopia. These include genital tract anomalies (50%), skeletal malformations (40%), and anorectal anomalies, such as imperforate anus (20%). Renal ectopia has been associated with several congenital syndromes, including thrombocytopenia with absent radius syn-

https://doi.org/10.5455/annalsmedres.2025.08.226

drome, caudal regression syndrome, and VACTERL [1,5].

While the relationship between renal ectopia and long-term renal dysfunction—such as hypertension, proteinuria, or chronic kidney disease—remains unclear, thorough evaluation and ongoing monitoring for associated anomalies are essential. This study aimed to evaluate the clinical presentation and associated abnormalities in children diagnosed with renal ectopia at a single tertiary care center.

MATERIALS AND METHODS

We retrospectively reviewed the medical records of 58 children with ectopic kidney disease who were followed in our department between January 2024 and June 2025. Patients' data, including age, gender, accompanying anomalies, laboratory findings, imaging results,and treatments, were retrospectively evaluated. The study was approved by the Scientific Research Evaluation and Ethics Committee of Gaziantep City Hospital (Number: 207/2025). All procedures were performed in accordance with the ethical standards and principles of the Declaration of Helsinki.

All ectopic kidneys were initially evaluated using ultrasonography (US). In a few patients whose kidneys were not visualized in the renal fossa on US, the ectopic kidney was subsequently confirmed by DMSA scintigraphy. Pelvic dilatation was graded according to the Society for Fetal Urology classification as follows: Grade 0, no dilation; Grade 1, mild dilation of the renal pelvis without calyceal involvement; Grade 2, mild dilation of the renal pelvis and a few calyces with normal renal parenchyma; Grade 3, moderate dilation of the renal pelvis and calyces with preserved renal parenchyma; Grade 4, severe dilation of the renal pelvis and calyces accompanied by thinning of the renal parenchyma [6].

Indications for voiding cystourethrogram (VCUG) included recurrent urinary tract infections ($\geq$2 episodes) or ultrasonographic findings suggestive of vesicoureteral reflux (VUR), such as hydronephrosis or ureteral dilatation. The International Reflux Study in Children system was used to grade VUR [7]. Indications for DMSA renal scintigraphy included the presence of VUR or recurrent urinary tract infections.

Urinary tract infection was defined as the growth of a single uropathogenic microorganism of $>10^5$ colony-forming units (CFU)/mL in a midstream urine sample or $>10^4$ CFU/mL in a catheterized urine sample [8]. If a random dipstick urinalysis was positive for protein ($\geq$1+), the protein/creatinine ratio in early morning urine was measured, and values >0.2 mg/mg were considered indicative of proteinuria [9].

Hypertension was defined as an average systolic or diastolic blood pressure $\geq 95^{th}$ percentile for sex, age, and height on at least three separate occasions or the use of antihypertensive drugs [10]. The estimated glomerular filtration rate (eGFR) was calculated using the Schwartz formula [11].

Statistical analysis

Statistical analyses were performed using the Statistical Package for the Social Sciences version 22. Continuous variables were expressed as mean ± standard deviation or median (range) as appropriate. Categorical variables are expressed as numbers and percentages.

RESULTS

A total of 58 patients, including 33 females (56.8%) and 25 males (43.1%), with a mean age of 71.6 ± 56.4 months and a mean follow-up duration of 21.6 ± 38.9 months, were included in the study. Prenatal diagnosis was made in 4 patients (6.8%) and postnatally in 54 patients. Consanguinity was present in 28 patients (48.2%), and a family history of congenital anomalies of kidney and urinary tract (CAKUT) was reported in 11 patients (18.9%).

Table 1. Socio-demographic data and urogenital system findings in children with ectopic kidney.

(n=58)	Mean±SD n (%)
Gender	
Female	33 (56.8)
Male	25 (43.1)
Timing of the diagnosis diagrenatal	4 (6.8%)
Postnatal	54 (93.1%)
Age (months)	71.6 ± 56.4
Follow-up duration (months)	11.6 ± 8.9
Consanguinity (n)	28 (48.2)
CAKUT family historyFamily history of CAKUT (n)	11 (18.9)

n: number of patients, SD: standard deviation, CAKUT: congenital anomalies of the kidney and urinary tract.

Table 2. Urogenital anomalies identified in patients with ectopic kidney disease.

Urogenital Anomaly	n (%)
Hydronephrosis	7 (12)
Vesicoureteral reflux	4 (6.8)
Neurogenic bladder	4 (6.8)
Duplicate collection system	3 (5.1)
Nephrolithiasis	2 (3.4)
Left undescended testicle	2 (3.4)
Hypospadias	1 (1.7)
Contralateral multicystic dysplastic kidney	1 (1.7)
Contralateral renal agenesis	1 (1.7)
Vesicostomy	1 (1.7)

Table 3. Laboratory data of the patients at presentation.

	Mean ± SD
Urea (mg/dl)	13±4.1
Creatinine (mg/dL)	0.56 ±0.6
Na (mmol/L)	135.6±4.2
K (mmol/L)	3.87 ±0.1
Al (mmol/L)	101.3±1.9
eGFR (mL/min/1.73 m^2)	112.2±13.4

https://doi.org/10.5455/annalsmedres.2025.08.226

Of the 58 patients, 26 (44.8%) and 32 (55.1%) had right and left renal ectopia, respectively. Crossed renal ectopia (CRE) was observed in 9 (15.5%) patients. Among these, 3 cases were right-sided CRE and 6 were left-sided CRE. Additionally, 7 patients with CRE had crossed-fused renal ectopia, of whom 3 had right-sided and 4 had left-sided crossed-fused renal ectopia. Table 1 presents the sociodemographic data and urogenital system findings.

Additional urogenital anomalies were identified as follows: hydronephrosis (n = 7), neurogenic bladder (n = 4), vesicoureteral reflux (VUR) (n = 3), duplicated collecting system (n = 3), nephrolithiasis (n = 2), left undescended testicle (n = 2), hypospadias (n = 1), contralateral multicystic dysplastic kidney (MCDK) (n = 1), contralateral renal agenesis (n = 1), and vesicostomy (n = 1). Additional urogenital anomalies are given in Table 2.

Eleven patients (18.9%) had additional abnormalities, including meningomyelocele (n = 3), anal atresia (n = 3), ventricular septal defect (VSD) (n = 2), cerebral palsy (n = 1), liver transplantation (n = 1), and Henoch-Schönlein purpura nephritis (HSP nephritis) (n=1).

Ten patients (17.2%) had a history of UTI. Voiding cystourethrography (VCUG) was performed in 12 (20%) patients. Of these, 1 patient had grade 5 vesicoureteral reflux (VUR) on the same side as the ectopic kidney, and 2 patients had bilateral grade 3 VUR.

Among the 58 patients, 53 (91.3%) underwent DMSA scintigraphy. Renal scarring was detected in 8 of these patients. Among the patients with scarring, 1 had hypertension, 1 had proteinuria, 1 was being followed-up with stage II chronic kidney disease (CKD), and 1 had stage 5 CKD. Table 3 summarizes the patients' laboratory parameters at presentation.

DISCUSSION

Renal ectopia was more frequently observed in females than males in our cohort, with a mean age at diagnosis of 71.6 ± 56.4 months. Prenatal detection was achieved in a minority of patients, which is lower than the 15%–20% rates reported in recent studies where widespread antenatal ultrasonography has improved early diagnosis [12,13]. This disparity may be attributed to regional demographics, as access to regular antenatal care and ultrasonographic screening can be limited by socioeconomic barriers and health care disruptions. Consanguinity was present in nearly half of our patients, similar to other Turkish cohorts investigating congenital anomalies of the kidney and urinary tract (CAKUT) [14]. In addition, a positive family history of CAKUT was reported in a subset of patients, supporting the role of genetic predisposition in the pathogenesis of renal ectopia [15,2].

Embryologically, fusion anomalies likely result from abnormal kidney migration and rotation during early gestation, and the predominance of fusion in CRE may be due to shared vascular and positional disturbances during renal ascent [3,4]. Left renal ectopia was more common than right renal ectopia, consistent with previous reports [1]. The proportion of crossed-fused renal ectopia among patients with CRE aligns with the findings of prior pediatric studies [3,16].

Additional urogenital anomalies were present in a considerable proportion of patients, with hydronephrosis being the most common finding, followed by neurogenic bladder, VUR, and duplicated collecting system. The coexistence of contralateral anomalies, such as MCDK or renal agenesis, may have implications for long-term renal function, particularly in patients with a solitary functioning kidney. Anomalies involving the lower urinary tract underline the importance of thorough urogenital evaluation, as timely detection and management may prevent further renal damage.

Systemic congenital anomalies were observed in a subset of patients, supporting the association between renal ectopia and multisystem congenital disorders, in line with previous reports [17].

VUR was identified in a subset of patients with renal scarring, highlighting its role in renal injury. Our findings suggest that the presence of hydronephrosis or a history of recurrent urinary tract infections may serve as predictive indicators for VUR. Therefore, VCUG may be considered selectively in patients with these risk factors rather than universally in all patients with ectopic kidneys.

Renal scarring emphasizes the increased risk of renal damage due to anatomical abnormalities. Careful follow-up and early detection of urological abnormalities are crucial in determining the long-term prognosis and guiding management.

The strengths of our study include a relatively large single-center pediatric cohort and comprehensive evaluation of associated anomalies.

Limitations

The limitations include its retrospective design and limited follow-up duration for some patients. Although all patients with renal scarring had VUR, the small number of events precluded formal statistical analysis to assess the association's strength or significance.

CONCLUSION

A careful and detailed physical examination is essential due to the frequent presence of additional congenital and urogenital anomalies. Early detection of urological abnormalities, such as vesicoureteral reflux (VUR), plays a crucial role in determining long-term prognosis and guiding management.

Ethics Committee Approval: The study was approved by the Scientific Research Evaluation and Ethics Committee of Gaziantep City Hospital (Number: 207/2025).

Informed Consent: Individual informed consent is not applicable for this study because no identifiable personal patient information was used.

https://doi.org/10.5455/annalsmedres.2025.08.226

Peer-review: Externally peer-reviewed.

Conflict of Interest: The authors have no conflicts of interest to declare.

Author Contributions: Conception: Z.A, E.O.C.D; Design: Z.A, E.O.C.D; Supervision: E.O.C.D; Materials: Z.A, E.O.C.D; Data Collection and/or Processing: Z.A; Analysis and/or Interpretation: Z.A, E.O.C.D; Literature Review: Z.A, E.O.C.D; Writing: Z.A; Critical Review: E.O.C.D.

Financial Disclosure: This study received no external funding.

Artificial Intelligence Disclosure: The authors declare that an artificial intelligence–based tool (ChatGPT, OpenAI, version GPT-4) was used solely for language editing and improving the clarity and readability of the manuscript. The AI tool did not contribute to the study design, data collection, data analysis, interpretation of results, or the formulation of scientific conclusions, and no original scientific content, clinical interpretation, or analytical reasoning was generated by the AI system. All content was critically reviewed, revised, and approved by the authors, who take full responsibility for the manuscript. We confirm that the use of artificial intelligence complies with the ethical standards and authorship policies of Annals of Medical Research.

REFERENCES

1. Jain A, Shrivastava A, Malik R. Ectopic kidney: a rare presentation. *Int J Sci Rep.* 2022;8(7):190-3. doi: 10.18203/issn.2454-2156.IntJSciRep20221590.
2. Rinat C, Farkas A, Frishberg Y. Familial inheritance of crossed fused renal ectopia. *Pediatr Nephrol.* 2001;16(3):269-70. doi: 10.1007/s004670000540.
3. Glodny B, Petersen J, Hofmann KJ, et al. Kidney fusion anomalies revisited: Clinical and radiological analysis of 209 cases of crossed fused ectopia and horseshoe kidney. *BJU Int.* 2009;103(2):224-35. doi: 10.1111/j.1464-410X.2008.07912.x.
4. Patel TV, Singh AK. Crossed fused ectopia of the kidneys. *Kidney Int.* 2008;73(5):662. doi: 10.1038/sj.ki.5002418.
5. Cunningham BK, Khromykh A, Martinez AF, et al. Analysis of renal anomalies associated with VACTERL association. *Birth Defects Res A Clin Mol Teratol.* 2014;100(10):801–805. doi: 10.1002/bdra.23302.
6. Fernbach SK, Maizels M, Conway JJ. Ultrasound grading of hydronephrosis: An introduction to the system used by the Society for Fetal Urology. *Pediatr Radiol.* 1993;23(6):478-80. doi: 10.1007/BF02012459.
7. Liebowitz RL, Olbing H, Parkkulainen KV, et al. International system of radiographic grading of vesicoureteric reflux. International Reflux Study in Children. *Pediatr Radiol.* 1985;15(2):105-9. doi: 10.1007/BF02388714.
8. Roberts KB. Subcommittee on Urinary Tract Infection, Committee on Quality Improvement Urinary tract infection: clinical practice guideline for the diagnosis and management of the initial UTI in febrile infants and children 2 to 24 months. *Pediatrics.* 2011;128(3):595-610. doi: 10.1542/peds.2011-1330.
9. National Kidney Foundation. K/DOQI Clinical Practice Guidelines for Chronic Kidney Disease: Evaluation, Classification, and Stratification. *Am J Kidney Dis.* 2002;39(2 Suppl 1):S1-266. PMID: 11904577.
10. Flynn JT, Kaelber DC, Baker-Smith CM, et al. Clinical Practice Guideline for Screening and Management of High Blood Pressure in Children and Adolescents. *Pediatrics.* 2017;140(3):e20171904. doi: 10.1542/peds.2017-1904.
11. Schwartz GJ, Muñoz A, Schneider MF, et al. New equations for estimating the GFR in children with CKD. *J Am Soc Nephrol.* 2009;20(3):629-37. doi: 10.1681/ASN.2008030287.
12. Shapiro E. Upper urinary tract anomalies and perinatal renal tumors. *Clin Perinatol*. 2014;41(3):679-94. doi: 10.1016/j.clp.2014.05.014.
13. Gică N, Apostol LM, Huluță I et al. Bilateral renal ectopia—prenatal diagnosis. *Diagnostics (Basel).* 2024;14(5):539. doi: 10.3390/diagnostics14050539.
14. Demir E, Çalışkan Y, Aliyeva N et al. Importance of Parental Consanguinity and Family History of Kidney Disease in the Turkish Adult Chronic Kidney Disease Population: An Epidemiologic Study. *Turk J Nephrol.* 2024;33(4):333-41. doi: 10.5152/turkjnephrol.2024.22442.
15. Sahin E, İnciser Paşalak Ş, Seven M. Consanguineous marriage and its effect on reproductive behavior and prenatal screening. *J Genet Couns.* 2020;29(5):849-856. doi: 10.1002/jgc4.1214.
16. Caffey's Pediatric Diagnostic Imaging, 2-VolumeSet, Edition 13. *Elsevier.* 2018.
17. Li ZY, Chen YM, Qiu LQ, et al. Prevalence, types, and malformations in congenital anomalies of the kidney and urinary tract in newborns: a retrospective hospital-based study. *Ital J Pediatr.* 2019;45(1):50. doi: 10.1186/s13052-019-0635-9.

https://doi.org/10.5455/annalsmedres.2025.08.226

Ann Med Res

Current issue list available at Ann Med Res

Annals of Medical Research

journal page: annalsmedres.org

The role of mood in complex regional pain syndrome: Cause or consequence?

Ozlem Kuculmez [a,*], Emine Dundar Ahi [b]

[a] Baskent University Alanya Hospital, Department of Physical Medicine and Rehabilitation, Antalya, Türkiye
[b] Kocaeli Health and Technology University, Faculty of Health Sciences, Department of Physiotherapy and Rehabilitation, Kocaeli, Türkiye
*Corresponding author: akanozlem07@gmail.com (Ozlem Kuculmez)

MAIN POINTS

- Anxiety and depression often accompany complex regional pain syndrome.
- It's unclear if this condition precedes or follows the disease.
- The study's results indicate that mood changes stem from the disease.

Cite this article as: Kuculmez O, Dundar Ahi E. The role of mood in complex regional pain syndrome: Cause or consequence?. *Ann Med Res*. 2026;33(2):60–66. doi: 10.5455/annalsmedres.2025.07.208.

ABSTRACT

Aim: Complex Regional Pain Syndrome (CRPS) involves pain and dysfunction in multiple nervous system pathways. Psychological symptoms such as anxiety, depression, and difficulty coping often accompany the physical aspects of the condition. This study sought to examine whether mood-related factors play a causal role in the onset of CRPS or if individuals with pre-existing psychological conditions exhibit increased susceptibility to its development.

Materials and Methods: This is a cross-sectional study that included 131 patients with a history of trauma or surgery who were referred for rehabilitation within the first three months following the incident. Among them, 70 patients were diagnosed with CRPS, while 61 patients formed the control group. Each participant underwent evaluation through the Short Form-36, Visual Analog Scale (VAS), Beck Depression Inventory, and the Beck Anxiety Inventory.

Results: The study included 62 men and 69 women, with no significant differences in anxiety and depression scores observed between the CRPS group and the control group ($p>0.05$ for both). However, individuals with CRPS reported notably higher scores on the VAS ($p<0.05$). In addition, their scores were significantly lower in the Short Form-36 subdomains related to pain intensity ($p<0.05$), social functioning ($p<0.05$), and physical role limitations ($p<0.05$).

Conclusion: The results indicate that an individual's baseline mood does not seem to contribute to the development of CRPS. These mood changes may be only the result of the disease, as pain level, social function, and physical role were determined to be worse in these patients.

Keywords: Anxiety, Complex regional pain syndrome, Depression, Mood, Reflex sympathetic dystrophy

Received: Jul 30, 2025 **Accepted:** Nov 04, 2025 **Available Online:** Feb 25, 2026

INTRODUCTION

Complex Regional Pain Syndrome (CRPS-I) typically emerges following an injurious event and is characterized by pain, edema, dysregulated cutaneous perfusion, and abnormal sudomotor activity [1]. CRPS frequently affects the upper or lower limbs and presents with a constellation of autonomic, sensory, and vasomotor abnormalities. Common clinical features include ongoing pain, changes in skin coloration and temperature, motor impairment, hypersensitivity, muscular and osseous wasting, excessive perspiration, and atypical patterns in hair and nail development [2].

The disease was reported to affect 13.6 individuals per 100,000 each year. It exhibits a higher prevalence in women and predominantly involves the upper limbs, often presenting with comorbidities distinct from those commonly seen in other chronic musculoskeletal conditions [3]. The diagnosis relies on the internationally endorsed Budapest criteria [4].

Beyond its physical manifestations, CRPS is strongly linked to psychological and emotional disturbances. Affected individuals commonly experience depression, anxiety, frustration, and difficulty coping factors that can heighten pain perception and impair daily functioning [5]. These emotional disturbances may not only be consequences of chronic pain but could also influence autonomic responses and central pain processing, potentially perpetuating the condition. Psychiatric comorbidities, such as mood disorders and somatic symptom presentations, are frequently observed in this population and may compromise therapeutic outcomes. However, it is not certain whether these psychological symptoms predate the onset of CRPS or develop as a result of the disease

and its disabling effects [6].

The literature reflects ongoing debate regarding the temporal relationship between mood disorders and CRPS. Some evidence suggests that pre-existing psychological vulnerabilities such as catastrophic thinking, high anxiety levels, or poor stress resilience may contribute to disease onset [7]. Conversely, other research proposes that psychiatric symptoms arise in response to the intense pain, limited mobility, and delayed recognition often associated with CRPS. Recent findings indicate a notable rise in psychological distress following diagnosis, particularly in patients with severe or persistent symptoms [8]. While the biopsychosocial framework is widely accepted as foundational for CRPS management, the precise influence of mental health variables on both disease development and progression remains insufficiently defined and continues to be a major area of investigation [7].

This study aims to examine the influence and predictive value of mood disturbances specifically anxiety and depression in individuals diagnosed with CRPS. By assessing whether these conditions precede or result from the syndrome in outpatient contexts, the research seeks to clarify the chronological and causal interplay between psychological distress and CRPS symptoms. Elucidating these dynamics may guide the development of holistic treatment strategies and targeted screening protocols, ultimately improving clinical outcomes by integrating physical and psychological approaches.

MATERIALS AND METHODS

This is a cross-sectional cohort study. Ethical approval was secured from the Institutional Review Board of Baskent University Hospital (Approval No: E-94603339-604.01-484842, dated 23.07.25). All participants provided written informed consent regarding participation and the use of their data. The study adhered to the ethical standards outlined in the Declaration of Helsinki.

Patient selection and sampling

Patients referred to the physiotherapy clinic between February 2023 and February 2025, following initial evaluation by the Department of Orthopedics and Traumatology for trauma-related conditions or postoperative care, were recruited for this study. An a priori power analysis was conducted using G*Power (version 3.1.9.4). Based on a medium effect size (d = 0.5) consistent with previous literature [7], a minimum of 51 participants per group (total N = 102) was required to achieve 80% statistical power at an alpha level of 0.05.

Inclusion and exclusion criteria

Participants who suffered from trauma or undergone surgical procedures were recruited within a three-month timeframe were evaluated for inclusion to the study. Individuals diagnosed with CRPS Type I based on the Budapest criteria were assigned to the CRPS group, while those exhibiting no clinical signs of CRPS were allocated to the control group. The primary objective of this study is to examine whether mood disturbances, such as anxiety and depression, predated the onset of complex regional pain syndrome or if they manifested subsequently as a consequence of the disease. Accordingly, only patients within the initial three months of the acute phase were included in the study cohort, given that in chronic cases, prolonged disease progression may render mood alterations an anticipated outcome.

Exclusion criteria included individuals under 18 or over 65 years of age, those with rheumatologic conditions, motor deficits, or myelopathy affecting the involved limb. Additionally, patients who had received injections, manual therapy, or physiotherapy in the affected area within the preceding three months; pregnant individuals; those demonstrating non-adherence to the treatment protocol; individuals with cognitive impairment; and those who were not willing to participate were excluded from the study cohort.

Evaluation of the participants

All assessments were conducted by a single experienced physiatrist to ensure consistency. Demographic characteristics were documented for each participant, and all individuals were instructed to accurately complete the following standardized instruments: the Visual Analog Scale (VAS), Beck Depression Inventory (BDI), Beck Anxiety Inventory (BAI), and the Short Form-36 (SF-36) Health Survey.

The Visual Analog Scale is a straightforward, widely utilized tool designed to quantify subjective pain intensity. It involves a 10-centimeter horizontal or vertical line anchored by descriptors at each end (0 indicating "no pain" and 10 indicating "the most severe pain"). Participants mark the point that best reflects their current pain intensity, and the distance from the "no pain" endpoint to the marked location is measured in centimeters or millimeters. The VAS is recognized for its simplicity, reproducibility, and minimal equipment requirements, and it has been validated as a reliable measure for both acute and chronic pain [9].

The Beck Anxiety Inventory is a self-report questionnaire designed to assess the frequency of anxiety symptoms using a 4-point Likert scale. Responses range from 0 ("not at all") to 3 ("severely"), with total scores spanning 0 to 63. Higher scores denote greater levels of anxiety. Turkish version of the BAI was validated by Ulusoy et al., making it suitable for clinical and research use in Turkish populations [10].

The Beck Depression Inventory consists of 21 items assessing various emotional and somatic symptoms of depression. Each item offers four graded response options, reflecting symptom severity. Participants are instructed to select responses that best represent their emotional state. Total scores are interpreted as follows: 0–9 indicates no depression; 10–18 suggests mild depression; 19–29 corresponds to moderate depression; and 30–63 indicates a high likelihood of severe de-

https://doi.org/10.5455/annalsmedres.2025.07.208

Table 1. Demographic characteristics of the participants.

		CPRS Group (n= 70)	Control Group (n= 61)
Age (mean ± SD)		46.51±13.57	42.24±14.60
		n (%)	n (%)
Gender	Female	39 (55.7)	30 (49.2)
	Male	31 (44.3)	31 (50.8)
Education	Illiterate	2 (2.9)	1 (1.6)
	Primary school	36 (51.4)	29 (47.5)
	Secondary school	12 (17.1)	8 (13.1)
	High school	9 (12.9)	13 (21.3)
	University	11 (15.7)	10 (16.4)
Occupation	Unemployed	2 (2.9)	0 (0)
	Worker	16 (22.9)	11 (18)
	Retired	8 (11.4)	7 (7)
	Desc worker	14 (20)	18 (29.5)
	Housewife	28 (40)	20 (32.8)
	Student	2 (2.9)	5 (8.2)
Localization	Upper extremity	42 (60)	0 (0)
	Lower extremity	28 (40)	0 (0)
Operation history		23 (32.8)	14 (23.0)
Trauma history		56 (80)	11 (18)
Psychiatric disease		7 (10)	5 (8.2)

CRPS: Complex regional pain syndrome.

Table 2

Value	P value
Gender[µ]	X^2 = 0.058, p = 0.455
Education[#]	0.729
Occupation[#]	0.399
Localization[#]	**0.001***
Operation history[µ]	X^2= 1.578, p = 0.209
History of trauma[#]	**0.001***
History of psychiatric disease[#]	0.877

[µ]Pearson Chi Square test, [#]Fisher's exact test, *p < 0.05 statistically significant.

pressive symptoms. BDI has been shown to be usable across diverse populations [11].

To evaluate health-related quality of life, the SF-36 Health Survey was administered. This instrument is one of the most extensively used general health status questionnaires and has been validated for use in Turkish populations. The SF-36 assesses nine domains: physical functioning, role limitations due to physical problems, bodily pain, general health perceptions, vitality, social functioning, emotional role limitations, mental health, and perceived changes in health over time. Higher subscale scores reflect better perceived health and well-being, while lower scores suggest diminished quality of life [12].

Statistical analysis

Statistical analyses were performed using IBM SPSS Statistics for Windows, Version 25.0 (IBM Corp., Armonk, NY, USA). Categorical variables were presented as frequencies (n) and percentages (%), while continuous variables were assessed for normality using the Shapiro–Wilk test. Normally distributed data were expressed as mean ± standard deviation (SD), whereas non-normally distributed data were summarized as median (minimum–maximum).

Due to the non-normal distribution of the data, the Mann–Whitney U test was used to compare anxiety, depression, and SF-36 scores between groups. Categorical comparisons were conducted using the Pearson chi-square (χ^2) test or Fisher's exact test. Effect sizes were calculated using the rank-biserial correlation. For all analyses, a p-value < 0.05 was considered statistically significant.

RESULTS

Demographic characteristics

The study population comprised 131 individuals (62 males, 69 females). Of these, 70 patients were diagnosed with Complex Regional Pain Syndrome (CRPS), while 61 individuals constituted the control group. The mean age of the participants was 44.53±14.17 years. The majority of participants had completed primary education. Regarding occupation, a significant proportion were housewives, while a considerable segment worked in labor-intensive jobs.Among patients with CRPS, approximately 60% reported a history of trauma or surgical intervention involving the upper extremities, whereas the remaining 40% presented with involvement of the lower extremities. Specifically, 32.8% of CRPS patients had a documented history of surgery, while a substantially larger proportion (80%) reported a prior traumatic injury. The demographic and sociodemographic profiles of the participants are summarized in Table 1.

https://doi.org/10.5455/annalsmedres.2025.07.208

Table 3. Comparison of anxiety, depression and quality of life parameters between complex regional pain syndrome group and control group.

Valuable	Median	Min-Max	u	Effect size#	p
VAS	3	0-10	550.5	0.742	0.001*
BDI	8	0-35	1890.5	0.115	0.258
BAI	7	0-44	2016.0	-0.056	0.582
PF	80	0-100	1827.0	-0.144	0.154
PH	25	0-100	1292.0	-0.395	0.001*
EP	66.7	0-100	1875.0	-0.122	0.214
Energy/Fatigue	60	15-100	1927.0	-0.097	0.336
EW	60	16-100	1887.0	-0.116	0.251
SF	75	12.5-100	1696.0	-0.206	0.041*
Pain	62	0-100	1673.5	-0.216	0.033*
General health	62	5-100	1979.5	-0.073	0.472
Health change	50	25-75	2085.0	0.023	0.801

[µ]Man-Witney U test, [#]Rank-Biserial Correlation, *p < 0.05 statistically significant. VAS: Visual Analog Score, BDI: Beck Depression Inventory, BAI: Beck Anxiety Inventory, PF: Physical functioning, PH: Role limitations due to physical health, EW: Emotional well-being, SF: Social function.

Comparisons of categorical variables

Comparative analysis revealed no statistically significant associations between the incidence of CRPS and gender, education level, occupation, history of surgery, or psychiatric comorbidities (p>0.05). In contrast, both the localization of the pathology (p=0.001) and a history of trauma (p=0.001) were significantly associated with a CRPS diagnosis. The details are summarized in Table 2.

Clinical and quality oflife outcomes

There were no statistically significant differences between the CRPS and control groups regarding anxiety (p=0.582) or depression (p=0.258) levels. However, patients with CRPS demonstrated significantly higher pain intensity according to VAS scores (p=0.001). Furthermore, specific subdomains of the SF-36 health survey—specifically bodily pain (p=0.033), social functioning (p=0.041), and physical role limitations (p=0.001)—were significantly more impaired in the CRPS group compared to controls. The remaining SF-36 subscales did not differ significantly between the groups (p > 0.05). Comparisons of anxiety, depression, and quality of life parameters are presented in Table 3.

DISCUSSION

In the current study, no statistically significant differences in anxiety or depression scores were observed between individuals diagnosed with CRPS and the control group. However, participants in the CRPS group reported significantly greater pain intensity, as measured by the Visual Analog Scale (VAS). Moreover, specific domains of the SF-36 survey—namely bodily pain, physical role limitations, and social functioning—were notably more impaired in the CRPS group, while the remaining subscales showed no significant between-group differences.

The mean age of patients in the CRPS cohort was 46.51 years, aligning closely with findings from Cave et al., who reported a mean age of 47.1 years in an 8-year longitudinal study [7]. Regarding anatomical distribution, 60% of CRPS patients in this study exhibited upper extremity involvement, which is consistent with the broader literature identifying the upper limbs as the most frequently affected region [3-7]. A female predominance was observed in the CRPS group (55.7% female vs. 44.3% male), consistent with earlier studies reporting higher incidence rates among females and frequent upper extremity involvement [3-13]. One plausible explanation is that women may engage more frequently in domestic labor that predisposes them to upper limb injuries, thereby increasing the risk of developing CRPS.

A significantly higher incidence of preceding trauma was noted in the CRPS group compared to controls. While the precise pathophysiological mechanisms underlying CRPS remain debated, numerous publications identify trauma as a primary precipitating factor—a relationship clearly observed in this investigation.

The relationship between CRPS and psychological factors remains controversial. A retrospective case-control study involving 186 CRPS patients and 697 matched controls found no substantial association between CRPS and psychological conditions such as anxiety or depression [13]. Similarly, a systematic review of 31 empirical studies—most rated as having low to moderate methodological rigor—suggested that higher-quality studies generally did not identify psychological traits (e.g., anxiety, depression, neuroticism) as predictors of CRPS. However, exposure to stressful life events appeared to increase risk, warranting more rigorous investigation [14].

It is important to note that this study assessed participants within three months of their CRPS diagnosis, corresponding to the acute phase of the disease. The timing of assessment is critical, as psychiatric comorbidities often emerge or intensify with chronicity. Many studies fail to specify the interval between diagnosis and study inclusion, a methodological limitation that obscures differences between early- and late-stage CRPS and complicates assessments of treatment efficacy [13,14].

Literature on the chronic phase presents a different picture. A 2017 prospective study reported that 38% of CRPS patients

https://doi.org/10.5455/annalsmedres.2025.07.208

screened positive for post-traumatic stress disorder (PTSD), with most cases predating CRPS onset. This suggests PTSD may be a predisposing factor, particularly as maladaptive coping mechanisms were found to correlate with PTSD severity [15]. In another study of 50 patients, 60% had a history of depression, 20% reported panic attacks, and 18% had experienced alcohol or substance use disorders [16]. A separate retrospective analysis of 64 CRPS patients similarly documented a higher prevalence of psychological disorders—including adjustment disorders, depression, substance misuse, and personality disorders—compared to patients with other chronic pain conditions [5].

Further research indicates that while pre-CRPS psychiatric rates may mirror the general population, these rates escalate following onset [8]. For instance, one study found that post-diagnosis, the incidence of psychiatric disorders rose by 76%, suggesting a significant psychosocial impact of the disease [8]. Rommel et al. found psychiatric comorbidities in 78% of CRPS cases, with adjustment disorders and major depression being the most frequent [17]. Additionally, psychosocial evaluations indicate that CRPS contributes to adverse psychological states and is associated with diminished quality of life and occupational functioning [18].

The relationship between mood and pain may be bidirectional or cyclothymic. Tajerian et al., in an experimental study on mice, demonstrated that neuropathic pain is retained through neuroplastic mechanisms, potentially precipitating mood alterations such as anxiety [19]. Pereira et al. conducted a one-year follow-up of CRPS patients and determined that mood disturbances were diagnosed with greater frequency in this cohort compared to patients without CRPS [20]. Brinkers et al. demonstrated that psychiatric conditions can influence pain perception in CRPS and found that both neuropathic pain and psychiatric disorders responded to similar psychotropic treatments [5].

Despite this evidence, our study found no significant difference in anxiety or depression scores. This discrepancy is likely attributable to the cross-sectional design and the restriction of our sample to the acute phase (first three months), whereas mood disorders may manifest more prominently as the condition becomes chronic. Consequently, multicenter cohort studies with extended longitudinal follow-up are warranted.

Recent studies exploring the link between anxiety and CRPS suggest biological and behavioral mechanisms underlying this relationship. Anxiety may exacerbate CRPS symptoms by enhancing systemic inflammation and promoting peripheral sensitization through elevated catecholamine levels. Additionally, anxiety is associated with altered brain processing that can lead to central sensitization, amplifying the subjective pain experience. Individuals with heightened anxiety may also exhibit greater attentional bias toward pain, increasing symptom intensity through hypervigilance and catastrophic interpretation [15,16].

Regarding functional outcomes, CRPS patients in the current study reported significantly greater pain intensity on the VAS, and their physical role functioning and social participation (SF-36) were more severely compromised than in controls. Possible explanations include the effects of limb immobilization, which can lead to hyperalgesia, trophic changes, vascular dysregulation, and cortical reorganization. Cognitive and perceptual factors may also play a role; uncertainty or misunderstanding about the nature of CRPS may foster negative health beliefs and perceptions of disability, further intensifying the experience of pain and limiting functional recovery [17,18].

Limitations

This study has several limitations. First, the cross-sectional design precludes any inference of causal relationships between CRPS and associated psychological or functional outcomes. Second, reliance on self-administered instruments such as the SF-36 and VAS introduces the potential for response bias. Third, the study did not comprehensively control for confounding variables, including concurrent medication use and coexisting medical conditions. Fourth, patients were recruited from a single center within a defined time frame, which may limit generalizability.

A significant challenge in this field is recruiting patients who meet strict inclusion criteria, as CRPS is relatively uncommon. This study was powered at 80%; however, a causal analysis would require a substantially larger sample size. Additionally, our study focused exclusively on the acute phase (within three months of diagnosis) to determine if emotional difficulties existed prior to the chronic progression of the syndrome. Future research should encompass personality assessments and longitudinal follow-up of chronic cases. Finally, similar to the review by Beerthuizen et al. [21], we found no direct association between psychological factors and CRPS. However, unlike their review, our study did not examine the impact of significant life events, representing an important area for future comprehensive investigation.

CONCLUSION

Although no significant differences in anxiety and depression were observed between CRPS patients and controls in the acute phase, those affected by CRPS experienced markedly greater pain intensity. Additionally, the CRPS cohort demonstrated significant deficits in domains related to pain severity, social functioning, and physical role performance. These results highlight the profound impact of CRPS on functional abilities and overall quality of life. The absence of significant differences in other SF-36 subscales suggests that the burden of CRPS is localized to specific facets of daily living. Targeted interventions addressing these functional impairments may enhance therapeutic outcomes and inform comprehensive, multidisciplinary management strategies.

https://doi.org/10.5455/annalsmedres.2025.07.208

Abbreviations

Complex Regional Pain Syndrome (CRPS)

VAS: Visual Analog Scale

BDI: Beck Depression Inventory

BAI: Beck Anxiety Inventory.

SF-36: Short Form-36

PF: Physical functioning

PH: Role limitations due to physical health

EP: Role limitations due to emotional problems

F: Fatigue

EW: Emotional well-being

SF: Social functioning

P: Pain

GH: General health

HC: Health change

PTSD: Post-traumatic stress disorder

Data Availability Statement: Data cannot be shared openly to protect study participant privacy. The datasets used and/or analyzed during the current study are available from the corresponding author on reasonable request.

Ethics Committee Approval: Ethical approval was obtained from the Baskent University Non-Interventional Clinical Research Ethics Committee (Decision No: E-94603339-604.01-484842; Date: 23.07.2025).

Informed Consent: Written informed consent was provided by all participants or their legal guardians.

Peer-review: Externally peer-reviewed.

Conflict of Interest: All authors have seen and agreed with the content of this manuscript, disclose no financial interests, and take full responsibility for the data and give consent for publication.

Author Contributions: Study Design: O.K, E.D.A; Collecting Data: O.K; Statistical Analysis: O.K; Detailed Review: O.K, E.D.A; Writing: O.K, E.D.A.

Financial Disclosure: The researchers did not take any funding for the study from any public or private organization.

Artificial Intelligence Disclosure: The authors declare that an artificial intelligence–based tool (ChatGPT, OpenAI, version [4.0]) was used solely for language editing and improving the clarity and readability of the manuscript. The AI tool did not contribute to the study design, data analysis, interpretation of results, or scientific conclusions. All content was critically reviewed and approved by the authors, who take full responsibility for the manuscript.

REFERENCES

1. Ferraro MC, O'Connell NE, Sommer C, Goebel A, Bultitude JH, Cashin AG, Moseley GL, McAuley JH. Complex regional pain syndrome: advances in epidemiology, pathophysiology, diagnosis, and treatment. *Lancet Neurol.* 2024;23(5):522-533. doi: 10.1016/S1474-4422(24)00076-0.
2. Kessler A, Yoo M, Calisoff R. Complex regional pain syndrome: An updated comprehensive review. *NeuroRehabilitation.* 2020;47(3):253-264. doi: 10.3233/NRE-208001.
3. Bruehl S. An update on the pathophysiology of complex regional pain syndrome. *Anesthesiology.* 2010;113(3):713-25. doi: 10.1097/ALN.0b013e3181e3db38.
4. Alshehri FS. The complex regional pain syndrome: Diagnosis and management strategies. *Neurosciences (Riyadh).* 2023;28(4):211-219. doi: 10.17712/nsj.2023.4.20230034.
5. Brinkers M, Rumpelt P, Lux A, Kretzschmar M, Pfau G. Psychiatric Disorders in Complex Regional Pain Syndrome (CRPS): The Role of the Consultation-Liaison Psychiatrist. *Pain Res Manag.* 2018;2018:2894360. doi: 10.1155/2018/2894360.
6. JR Scarff. Managing Psychiatric Symptoms in Patients with Complex Regional Pain Syndrome. *Innov Clin Neurosci.* 2022;19(1-3):56-59. PMID: 35382068.
7. Cave SA, Reynolds LM, Tuck NL, Aamir T, Lee AC, Bean DJ. Anxiety, Disability, and Pain Predict Outcomes of Complex Regional Pain Syndrome: An 8-year Follow-up of a Prospective Cohort. *J Pain.* 2023;24(11):1957-1967. doi: 10.1016/j.jpain.2023.06.003.
8. Parinder A, Lyckegård Finn E, Dahlin LB, Nyman E. Associated factors, triggers and long-term outcome in Complex Regional Pain Syndrome (CRPS) in the upper limb - A descriptive cross-sectional study. *PLoS One.* 2025;20(3):e0320263. doi: 10.1371/journal.pone.0320263.
9. Price DD, McGrath PA, Rafii A, Buckingham B. The validation of visual analogue scales as ratio scale measures for chronic and experimental pain. *Pain.* 1983;17(1):45-56. doi: 10.1016/0304-3959(83)90126-4.
10. Ulusoy M, Sahin N, Erkmen H. Turkish Version of the Beck Anxiety Inventory: Psychometric properties. *Journal of Cognitive Psychotherapy.* 1998;12.2:163.
11. Hisli Sahin. N. A reliability and validity study of Beck Depression Inventory in a university student sample. *Türk Psikoloji Dergisi.* 1989;7.23:3-13.
12. Demiral Y, Ergor G, Unal B, Semin S, Akvardar Y, Kivircik B, Alptekin K. Normative data and discriminative properties of short form 36 (SF-36) in Turkish urban population. *BMC Public Health.* 2006;6:247. doi: 10.1186/1471-2458-6-247.
13. Borchers AT, Gershwin ME. Complex regional pain syndrome: A comprehensive and critical review. *Autoimmun Rev.* 2014;13(3):242–265. doi: 10.1016/j.autrev.2013.10.006.
14. Zalewski A, Andreieva I, Wiśniowska J, Tarnacka B, Gromadzka G. Clinical and Molecular Barriers to Understanding the Pathogenesis, Diagnosis, and Treatment of Complex Regional Pain Syndrome (CRPS). *Int J Mol Sci.* 2025;26(6). doi: 10.3390/ijms26062514.
15. Ziegler MG. Psychological Stress and the Autonomic Nervous System. Primer on the Autonomic Nervous System. *Academic Press.* 2012;291–293. doi: 10.1016/B978-0-12-386525-0.00061-5.
16. Ploghaus A, Narain C, Beckmann CF, Clare S, Bantick S, Wise R, Matthews PM, Nicholas P Rawlins J, Tracey I. Exacerbation of Pain by Anxiety Is Associated with Activity in a Hippocampal Network. *J Neurosci.* 2001;21(24):9896–9903. doi: 10.1523/JNEUROSCI.21-24-09896.2001.
17. Wolter T, Knöller SM, Rommel O. Complex regional pain syndrome following spine surgery: clinical and prognostic implications. *Eur Neurol.* 2012;68(1):52-8. doi: 10.1159/000337907.
18. Pepper A, Li W, Kingery WS, Angst MS, Curtin CM, Clark JD. Changes Resembling Complex Regional Pain Syndrome Following Surgery and Immobilization. *J Pain*. 2013;14(5):516–524. doi: 10.1016/j.jpain.2013.01.004.
19. Tajerian M, Leu D, Zou Y, Sahbaie P, Li W, Khan H, Hsu V, Kingery W, Huang TT, Becerra L, Clark JD. Brain neuroplastic changes accompany anxiety and memory deficits in a model of complex regional pain syndrome. *Anesthesiology.* 2014;121(4):852-65. doi: 10.1097/ALN.0000000000000403.

https://doi.org/10.5455/annalsmedres.2025.07.208

20. Pereira DE, Momtaz D, Gonuguntla R, Mittal M, Singh A, Dave D, Hosseinzadeh P. Patients With Preexisting Anxiety and Mood Disorders Are More Likely to Develop Complex Regional Pain Syndrome After Fractures. *Clin Orthop Relat Res.* 2024;482(2):222-230. doi: 10.1097/CORR.0000000000002957.

21. Beerthuizen A, van 't Spijker A, Huygen FJ, Klein J, de Wit R. Is there an association between psychological factors and the Complex Regional Pain Syndrome type 1 (CRPS1) in adults? A systematic review. *Pain.* 2009;145(1-2):52-9. doi: 10.1016/j.pain.2009.05.003.

https://doi.org/10.5455/annalsmedres.2025.07.208

Ann Med Res

Current issue list available at Ann Med Res

Annals of Medical Research

journal page: annalsmedres.org

Volumetric MRI analysis of the pineal gland and brain ventricles in patients with migraine

Ahmet Payas [a,*], Hamit Aksoy [b], Şule Göktürk [c], Yasin Göktürk [c], Hasan Yıldırım [d], Hikmet Kocaman [e]

[a]Amasya University, Faculty of Medicine, Department of Anatomy, Amasya, Türkiye
[b]Hitit University, Vocational School of Sungurlu, Computer Technologies Department, Çorum, Türkiye
[c]Kayseri City Training and Research Hospital, Department of Neurosurgery, Kayseri, Türkiye
[d]Karamanoğlu Mehmetbey University, Kamil Özdağ Faculty of Science, Department of Data Science and Analytics, Karaman, Türkiye
[e]Karamanoğlu Mehmetbey University, Faculty of Health Sciences, Department of Physiotherapy and Rehabilitation, Karaman, Türkiye
*Corresponding author: fizyopayass@gmail.com (Ahmet Payas)

MAIN POINTS

- Individuals with migraine have significantly smaller pineal gland and cerebral ventricle volumes compared to healthy controls.
- A smaller pineal gland volume may indicate reduced melatonin production capacity, potentially contributing to migraine pathophysiology.
- The reduction in third ventricle volume may be associated with increased intracranial pressure and decreased CSF-mediated melatonin transport.
- The study demonstrates that migraine is associated not only with functional but also with microstructural brain alterations.

Cite this article as: Payas A, Aksoy H, Göktürk Ş, Göktürk Y, Yıldırım H, Kocaman H. Volumetric MRI analysis of the pineal gland and brain ventricles in patients with migraine. *Ann Med Res*. 2026;33(2):67–72. doi: 10.5455/annalsmedres.2025.08.230.

ABSTRACT

Aim: Previous studies have reported reduced melatonin levels and elevated cerebrospinal fluid (CSF) pressure in patients with migraine. However, the volumetric characteristics of the pineal gland, which is the primary source of melatonin, and the brain ventricles, which serve as CSF reservoirs, have not been sufficiently investigated. This study analyzed the volumes of the pineal gland and brain ventricles in migraine patients.

Materials and Methods: The study included 21 migraine patients and 22 age- and sex-matched healthy controls. Brain volumetric analyses were performed using high-resolution magnetic resonance imaging (MRI). Pineal gland volumes were manually segmented and measured using ITK-SNAP software, while ventricular volumes were automatically computed using volBrain software. All volumetric measurements were expressed in cubic centimeters (cm^3).

Results: The groups were comparable in terms of age ($p=0.730$), gender ($p=0.420$), and body mass index ($p=0.082$). Pineal gland volume was significantly reduced in the migraine group. An ANCOVA controlling for total intracranial volume confirmed this significant reduction ($F(1, 39) = 34.95$, $p<0.001$, partial $\eta^2 = 0.473$). Likewise, ventricular volumes were significantly smaller in migraine patients ($p<0.001$).

Conclusion: These findings indicate that the reduction in pineal gland volume in migraine patients occurs independently of overall brain size, pointing to a specific structural change relevant to the underlying pathology of the disease.

Keywords: Pineal gland, Cerebral ventricles, Migraine, Headache

Received: Aug 19, 2025 **Accepted:** Nov 04, 2025 **Available Online:** Feb 25, 2026

INTRODUCTION

Migraine is a neurological disorder that affects approximately 15% of the global population and may occur at any age [1]. It is more prevalent among women and individuals under the age of 50, tends to follow a chronic course, and typically lasts between 4 hours and 3 days [2,3]. Migraine manifests primarily as a headache and is frequently accompanied by symptoms such as photophobia, phonophobia, nausea, or vomiting [1].

Despite the considerable individual and societal burden of migraine, its pathophysiology remains incompletely understood. While various theories have been proposed, neuroimaging studies have consistently revealed both structural and functional alterations in the brains of individuals with migraine [4,5,6]. Among these findings, the observation of reduced melatonin levels and elevated cerebrospinal fluid (CSF) pressure in migraine patients has drawn increasing attention.

The pineal gland, located above the thalamus, is responsible for the secretion of several hormones, most notably mela-

tonin [7]. Melatonin, one of the most potent natural antioxidants, can readily cross cellular membranes to neutralize reactive oxygen and nitrogen species, thereby reducing oxidative stress [8]. Emerging evidence suggests that melatonin plays a role in the pathophysiology of both primary and secondary headache disorders [9,10,11], and studies have consistently reported lower melatonin levels in individuals with migraine [8].

Melatonin secretion has been shown to be positively correlated with the volume of the pineal gland, and inter-individual differences in this volume may influence circulating melatonin levels [12,13]. Additionally, the cerebral ventricles—cavities within the central nervous system—are responsible for the production and circulation of CSF [14]. Several studies have suggested a potential link between ventricular system morphology and migraine pathophysiology, particularly regarding CSF dynamics [15,16]. Furthermore, it has been demonstrated that a large portion of melatonin secreted by the pineal gland enters the third ventricle directly through the pineal recess, suggesting that the ventricular system may be indirectly influenced by melatonin levels [17,18].

Although various theories exist regarding migraine pathogenesis, volumetric studies focusing on the pineal gland and cerebral ventricles remain limited. Given the evidence of low melatonin levels and increased CSF pressure in individuals with migraine, investigating the structural characteristics of these regions is warranted. Therefore, the aim of this study was to examine possible volumetric differences in the pineal gland and cerebral ventricles between migraine patients and healthy controls using magnetic resonance imaging (MRI).

MATERIALS AND METHODS

Study design and ethical considerations

This a cross-sectional cohort study conducted in a single center and adhered to the Declaration of Helsinki for scientific and ethical conduct in scientific research. Written informed consent was obtained from the participants. The study was approved by the institutional review board on February 28, 2024 (Institutional Review Board of Hitit University, Decision No. 2024-04).

Study groups

The study included a Migraine Group of 21 patients (15 females, 6 males) and a Control Group of 22 healthy, asymptomatic individuals (18 females, 4 males).

Inclusion and exclusion criteria

Migraine patients were selected based on the International Headache Society diagnostic criteria for migraine without aura. These criteria included: (I) headache attacks lasting 4–72 hours (untreated or unsuccessfully treated); (II) unilateral, pulsating pain of moderate to severe intensity; (III) aggravation by routine physical activity; (IV) associated nausea/vomiting or photophobia/phonophobia; and (V) the absence of other underlying diseases.

General inclusion criteria for all participants required that they be between 18 and 65 years of age, have a normal neurological examination, and show no lesions or anomalies on brain MRI. Participants were required to have no systemic diseases affecting the autonomic nervous system, no history of alcohol or substance abuse in the last five years, and no regular medication use for at least one month prior to the study. Individuals with neurodegenerative diseases, congenital brain anomalies, or a history of head trauma were excluded.

Image acquisition

Radiological evaluation of brain structures and the pineal gland was performed using a 3-Tesla MRI scanner (Magnetom Skyra, Siemens). The pineal gland was localized by identifying the corpus callosum, superior colliculus, third ventricle (ventriculus tertius), and quadrigeminal cistern. A T1-weighted MPRAGE sequence was acquired with the following parameters: sagittal plane, slice thickness = 1 mm, flip angle = 9°, voxel size = 1 × 1 × 1 mm, repetition time (TR) = 2300 ms, field of view (FOV) = 250 × 250 mm^2, echo time (TE) = 3.4 ms, and matrix = 256 × 256.

Pineal gland volumetry

Pineal gland volumes were measured using ITK-SNAP software (Insight Segmentation and Registration Tool Kit). Manual segmentation was performed to ensure accuracy. Brain MRI data in DICOM format were imported into ITK-SNAP, and the boundaries of the pineal gland were delineated in the coronal, sagittal, and axial planes. Using the 'Active Label' and 'Interpolate Labels' tools, the gland boundaries were traced across all relevant slices. Upon completion of the segmentation, the software automatically calculated the pineal gland volume in cubic centimeters (cm^3) (Figure 1).

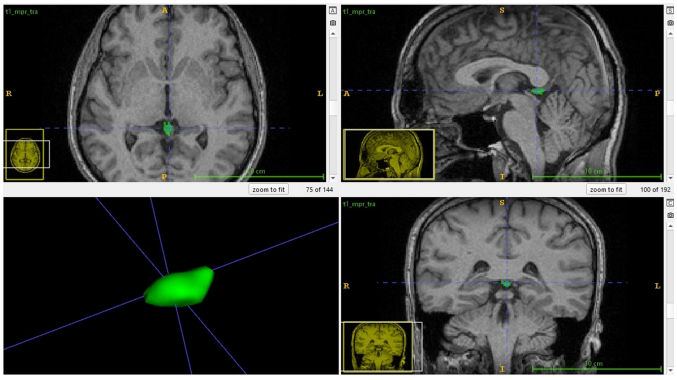

Figure 1. Pineal gland image reconstructed in ITK-SNAP program.

Brain ventricular volumetry

Brain ventricular volumes were calculated using the automated cloud-based volumetry system, volBrain (https://volbrain.upv.es). T1-weighted images were first converted from

https://doi.org/10.5455/annalsmedres.2025.08.230

DICOM to NIfTI format using dcm2niigui software and compressed into .zip archives. The data were then uploaded to the volBrain server. The 'vol2Brain' pipeline was selected, and participant demographic data (age and sex) were entered into the system. The server processed the data and generated a report detailing the volumetric information of the brain ventricles (Figure 2).

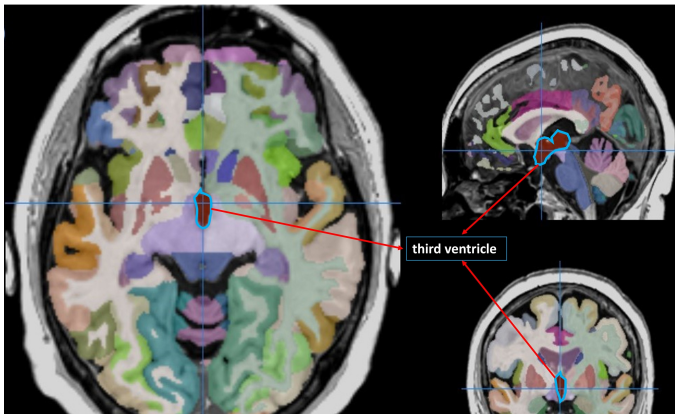

Figure 2. Brain ventricle images reconstructed in volBrain program.

Statistical analysis

Statistical analyses were conducted using IBM SPSS Statistics (Version 22.0; IBM Corp., Armonk, NY, USA), R (Version 4.4.3), and JASP (Version 0.19.3). Continuous variables were expressed as mean and standard deviation (Mean ± SD), while categorical data were presented as frequencies (n) and percentages (%). Group comparisons for baseline characteristics were performed using the independent samples t-test for continuous variables and the Pearson chi-squared test for categorical variables.

To assess differences in pineal gland volume between migraine patients and healthy controls while accounting for variations in overall brain size, Analysis of Covariance (ANCOVA) was employed. Total intracranial cavity volume was included as a covariate to isolate the effect of group status. Model assumptions were rigorously verified: linearity was assessed via scatterplots; homogeneity of regression slopes was confirmed by the non-significant interaction between Group and Intracranial Cavity; normality of residuals was checked using Q-Q plots and the Shapiro-Wilk test; and homogeneity of variance was assessed using Levene's test.

A post-hoc power analysis was conducted using G*Power (version 3.1.9.7) to evaluate sample size adequacy. The analysis indicated a high statistical power ($1-\beta = 0.99$) to detect the observed effect size [$f = 0.94$] at $\alpha = 0.05$. Statistical significance was defined as $p<0.05$.

RESULTS

Demographics and initial comparisons

Table 1 summarizes the demographic characteristics and initial volumetric measurements. There were no statistically significant differences between the groups regarding gender distribution (p=.420), mean age (t(41) = -0.35, p=.730), or Body Mass Index (t(41) = -1.78, p=.082), confirming the comparability of the two cohorts.

Volumetric analysis

Volumetric comparisons, summarized in Table 2, revealed distinct structural differences. The migraine group exhibited a significantly smaller pineal gland volume, which was approximately 23% smaller than that of the control group (p<.001). A consistent reduction was also observed across the ventricular system; volumes of the lateral ventricle (p<.001), third ventricle (p<.001), and fourth ventricle (p=.005) were all significantly smaller in migraine patients. Conversely, while the total volumes of Grey Matter, White Matter, and the overall Intracranial Cavity were slightly smaller in the migraine group, these differences were not statistically significant (p=.961 and p=.791, respectively). This indicates that the observed volumetric reductions are specific to the pineal-ventricular system rather than a consequence of global differences in brain or head size.

Results of ANCOVA

As detailed in Table 3, Analysis of Covariance (ANCOVA) was performed to determine if the difference in pineal gland volume persisted after accounting for intracranial cavity volume (ICV). Prior to analysis, all assumptions were verified. The assumption of homogeneity of regression slopes was met, as the interaction between group status and ICV was not statistically significant ($F(1, 39) = 0.237$, p=.629, partial η^2 =.006), confirming that the relationship between ICV and pineal volume was consistent across groups. Levene's test for homogeneity of error variances was also non-significant ($F(1, 41) = 0.351$, p=.557). Additionally, standardized residuals were normally distributed with no significant outliers.

After adjusting for ICV, the ANCOVA revealed a significant main effect of group status ($F(1, 39) = 34.95$, p<.001). The effect size was large (partial $\eta^2 = .473$), indicating that 47.3% of the variance in pineal gland volume was attributable to group differences after controlling for brain size.

Analysis of means

Unadjusted descriptive statistics showed a mean pineal gland volume of 0.20 cm^3 (SD=0.03) for the migraine group and 0.26 cm^3 (SD=0.04) for the control group. After controlling for ICV, the adjusted means (estimated marginal means) remained 0.20 cm^3 and 0.26 cm^3, respectively. Pairwise comparisons confirmed that the control group had a significantly larger pineal gland volume, with a mean difference of 0.058 cm^3 (95% CI: 0.038 to 0.078, p<.001). The minimal difference between unadjusted and adjusted means suggests that the reduction in pineal volume in migraine patients is a robust finding, independent of intracranial cavity volume.

https://doi.org/10.5455/annalsmedres.2025.08.230

Table 1. Descriptive statistics of the participants.

	Migraine group (n=21) (Mean±SD)	Control group (n=22) (Mean±SD)	Sig. (p)
Gender F/M (F% / M%)	15/6 (71.43% / 28.57%)	18/4 (81.2582% / 18.18%)	0.420
Age (years)	37.86±6.75	38.55±6.22	0.730[a]
BMI	26.42±1.64	27.48±2.25	0.082[b]

SD: Standard deviation, BMI: Body mass index, [a]: t-test, [b]: Welch t-test.

Table 2. Comparison of pineal gland and brain ventricle volume data between groups.

	Migraine group (n=21) (Mean±SD)	Control group (n=22) (Mean±SD)	Sig. (p)
Pineal gland volume (cm^3)	0.20±0.018	0.26±0.036	**p<0.001[a]**
Lateral ventricle volume (cm^3)	7.65±2.39	15.63±6.80	**p<0.001[b]**
Third ventricle volume (cm^3)	0.76±0.33	1.32±0.55	**p<0.001[b]**
Fourth ventricle volume (cm^3)	1.12±0.511	1.52±0.37	**0.005[a]**
Grey and White Matter (cm^3)	1135.98±96.07	1136.55±100.54	0.961[b]
Intracranial Cavity (cm^3)	1306.99±86.26	1313.27±96.99	0.791[a]

SD: Standard deviation, [a]: t-test, [b]: Welch t-test.

Table 3. Analysis of Covariance (ANCOVA) for the effects of group and intracranial cavity volume on pineal gland volume.

Source	SS	df	MS	F	Sig. (p)[c]	η^2
ANCOVA Model						
Group (Main Effect)	0.036	1	0.036	34.951	**<0.001**	0.473
Intracranial Cavity (Covariate)	0.001	1	0.001	0.750	0.392	0.019
Assumption Test						
Group x Intracranial Cavity	0.00025	1	0.00025	0.237	0.629	0.006
Error	0.040	39	0.001			

SS: Sum of Squares, MS: Mean Square, Model R Squared = 0,478 (Adjusted R Squared = 0.438), [c]: Analysis of covariance test. Note. The main effect of Group is interpreted as the interaction term was not significant.

DISCUSSION

This study demonstrated that individuals with migraine have significantly smaller pineal gland and cerebral ventricle volumes compared to healthy controls. These findings may be associated with the reduced melatonin levels and increased intracranial pressure frequently observed in migraine patients. Although multiple theories have been proposed regarding the pathophysiology of migraine, the role of reduced melatonin levels has recently attracted significant attention [19,6].

Located above the thalamus, the pineal gland plays a key role in regulating the body's physiological and circadian rhythms [8]. In addition to glial cells, the pineal gland contains endocrine cells known as pinealocytes, which are of photoreceptor origin and are responsible for synthesizing hormones, particularly melatonin [20]. Melatonin is one of the most potent natural antioxidants, capable of easily diffusing across cell membranes to neutralize reactive oxygen and nitrogen species [8].

The pineal gland's involvement in migraine is supported by studies demonstrating that melatonin supplementation reduces headache frequency and intensity [9,10,11]. In an experimental study, Tanuri et al. (2009) showed that rats subjected to pinealectomy exhibited increased c-fos positive cells associated with pain, and that melatonin administration significantly reduced the number of these cells [21]. Other animal studies have reported that melatonin modulates pain by reducing neuroinflammation [22,23].

Previous research has consistently shown that individuals with migraine tend to have lower melatonin levels [8,9,10,11]. These biochemical differences may be linked to the structural characteristics of the pineal gland, as melatonin secretion has been found to correlate with pineal volume [12,24]. Studies suggest that in healthy adults aged 25–65, the average pineal volume ranges between 0.22–0.24 cm^3 [25,26]. In the present study, the average pineal volume was 0.24 cm^3 in the control group compared to 0.19 cm^3 in the migraine group. This reduction in volume may reflect a diminished capacity for melatonin production, potentially contributing to the low melatonin levels reported in this population.

The cerebral ventricles—cavities within the central nervous system—play a crucial role in the production and circulation of cerebrospinal fluid (CSF) [14]. Beyond providing mecha-

https://doi.org/10.5455/annalsmedres.2025.08.230

nical protection, the ventricles help maintain brain homeostasis by clearing metabolic waste and regulating CSF composition. Several studies suggest a potential link between CSF dynamics and migraine pathophysiology [15,16]. For instance, Chen et al. found a reduction in fourth ventricle volume in individuals with episodic migraine. Although we did not directly measure CSF pressure, alterations in ventricular volume may indirectly reflect changes in intracranial pressure [27].

While some studies have reported that longer migraine duration is associated with increased CSF volumes in the lateral and third ventricles, hinting at intracranial hypertension, our findings differ. Notably, although migraine and idiopathic intracranial hypertension share common risk factors, their pathophysiological mechanisms are distinct [15,16].

In our study, the reduced ventricular volumes observed in migraine patients may indicate restricted physical space for CSF, potentially leading to increased CSF pressure despite the smaller volume. The third ventricle is particularly significant in this context. The pineal gland, situated just above the roof of the third ventricle, secretes melatonin directly into the CSF via the pineal recess [28,29]. Consequently, melatonin concentrations in the ventricular system may be higher than in peripheral blood. CSF-delivered melatonin may suppress the activity of the trigeminovascular system, a key pathway in migraine pathogenesis [30,31]. Trigeminal neurons, similar to visceral sensory neurons, innervate the meninges and are directly involved in pain transmission [12,29,32]. In this study, the third ventricle volume in migraine patients was approximately 44% smaller than in controls. This reduction, combined with decreased pineal volume, may result in lower local melatonin concentrations and subsequent disinhibition of the trigeminovascular system, contributing to headache severity.

The cross-sectional design of the present study precludes establishing a causal relationship between reduced pineal gland volume and migraine. It remains uncertain whether the observed volumetric reduction represents a predisposing structural vulnerability contributing to migraine onset or a secondary adaptation resulting from the chronic course of the disorder. Previous neuroimaging studies have shown that prolonged pain exposure and recurrent nociceptive activation can induce microstructural and volumetric alterations in brain regions associated with pain modulation and circadian regulation [33,34]. Similarly, long-term alterations in melatonin secretion secondary to repeated attacks could lead to pineal gland remodeling or atrophy over time [8,28]. Therefore, the reduced pineal volume observed here likely reflects a complex interaction between predisposing neuroendocrine dysregulation and chronic disease-related neuroplasticity. Longitudinal studies integrating volumetric, biochemical, and clinical data are required to disentangle this bidirectional relationship.

Neuroimaging has previously revealed functional and microstructural alterations in migraine patients, particularly in pain processing regions such as the brainstem, hypothalamus, basal ganglia, and cerebral cortex [27,33,34]. The present study suggests that the pineal gland and cerebral ventricles should be added to the list of structures undergoing microstructural changes in the migraine brain.

Limitations

This study has several limitations. First, only patients with migraine without aura were included; future studies should examine different migraine subtypes. Second, the sample size was relatively small; however, a post-hoc analysis indicated sufficient statistical power for the main outcome. Third, although we attempted to control for confounding variables, factors such as lifestyle, medication use, and genetic predisposition were not comprehensively analyzed. Lastly, the study relied solely on volumetric MRI data; integrating functional imaging and biochemical markers would provide a more comprehensive understanding of structural-functional correlations. Addressing these limitations in future research will strengthen the clinical implications of these findings.

CONCLUSION

These findings demonstrate that individuals with migraine have significantly smaller pineal gland and cerebral ventricle volumes compared to healthy controls. Notably, the reduction in pineal gland volume appears to be independent of overall brain size, suggesting a specific structural alteration in the migraine brain that may contribute to the underlying pathophysiology of the disorder.

Ethics Committee Approval: Ethical approval was obtained from the Institutional Review Board of Hitit University, Çorum, Turkey (Date: February 28, 2024; Decision No: 2024-04).

Informed Consent: Written informed consent was obtained from each patient.

Peer-review: Externally peer-reviewed.

Conflict of Interest: The authors have no conflict of interest to declare.

Author Contributions: AP: Conception, Design, Supervision, Fundings, Materials, Data Collection and/or Processing, Analysis and/or Interpretation, Literature Review, Writing, Critical Review. HA: Fundings, Materials, Data Collection and/or Processing, Analysis and/or Interpretation, Literature Review. ŞG: Materials, Data Collection and/or Processing, Analysis and/or Interpretation, Literature Review. YG: Materials, Data Collection and/or Processing, Analysis and/or Interpretation, Literature Review. HY: Materials, Data Collection and/or Processing, Analysis and/or Interpretation, Literature Review, Writing. HK: Materials, Data Collection and/or Processing, Analysis and/or Interpretation, Literature Review, Writing, Critical Review.

https://doi.org/10.5455/annalsmedres.2025.08.230

Financial Disclosure: This study was not supported by any public, commercial, or not-for-profit funds for the conduct of research, study design, collection, analysis, and interpretation of the data writing the report, and/or decision of the article for publication.

Artificial Intelligence Disclosure: The authors declare that an artificial intelligence–based tool (ChatGPT, version 5.2) was used solely for language editing and improving the clarity and readability of the manuscript. The AI tool did not contribute to the study design, data analysis, interpretation of results, or scientific conclusions. All content was critically reviewed and approved by the authors, who take full responsibility for the manuscript.

REFERENCES

1. Dourson AJ, Darken RS, Baranski TJ, Gereau RW, Ross WT, Nahman-Averbuch H. The role of androgens in migraine pathophysiology. *Neurobiol Pain.* 2024;16:100171. doi: 10.1016/j.ynpai.2024.100171.
2. Ashina M, Katsarava Z, Do TP, et al. Migraine: epidemiology and systems of care. *Lancet.* 2021;397(10283):1485-1495. doi: 10.1016/S0140-6736(20)32160-7.
3. MacGregor EA. Migraine. *Ann Intern Med.* 2017;166(7):ITC49-ITC64. doi: 10.7326/AITC201704040.
4. Baksa D, Gonda X, Eszlari N, et al. Financial Stress Interacts With CLOCK Gene to Affect Migraine. *Front Behav Neurosci.* 2020;13:284. doi: 10.3389/fnbeh.2019.00284.
5. Kogelman LJA, Falkenberg K, Buil A, et al. Changes in the gene expression profile during spontaneous migraine attacks. *Sci Rep.* 2021;11(1):8294. doi: 10.1038/s41598-021-87503-5.
6. Rathnasiri Bandara SM. Paranasal sinus nitric oxide and migraine: a new hypothesis on the sino rhinogenic theory. *Med Hypotheses.* 2013;80(4):329–340. doi: 10.1016/j.mehy.2012.12.001.
7. Kumar V. Biological timekeeping: Clocks, rhythms and behaviour. *New Delhi: Springer India.* 2017;643–658. doi: 10.1007/978-81-322-3688-7.
8. Cipolla-Neto J, Amaral FGD. Melatonin as a Hormone: New Physiological and Clinical Insights. *Endocr Rev.* 2018;39(6):990-1028. doi: 10.1210/er.2018-00084.
9. Gonçalves AL, Martini Ferreira A, Ribeiro RT, Zukerman E, Cipolla-Neto J, Peres MF. Randomised clinical trial comparing melatonin 3 mg, amitriptyline 25 mg and placebo for migraine prevention. *J Neurol Neurosurg Psychiatry.* 2016;87(10):1127-1132. doi: 10.1136/jnnp-2016-313458.
10. Masruha MR, de Souza Vieira DS, Minett TS, et al. Low urinary 6-sulphatoxymelatonin concentrations in acute migraine. *J Headache Pain.* 2008;9(4):221-224. doi: 10.1007/s10194-008-0047-5.
11. Zduńska A, Cegielska J, Domitrz I. The Pathogenetic Role of Melatonin in Migraine and Its Theoretic Implications for Pharmacotherapy: A Brief Overview of the Research. *Nutrients.* 2022;14(16):3335. doi: 10.3390/nu14163335.
12. Batın S, Ekinci Y, Gürbüz K, et al. The role of pineal gland volume in the development of scoliosis. *Eur Spine J.* 2023;32(1):181-189. doi: 10.1007/s00586-022-07452-z.
13. Cipolla-Neto J, Amaral FG, Afeche SC, Tan DX, Reiter RJ. Melatonin, energy metabolism, and obesity: a review. *J Pineal Res.* 2014;56(4):371-381. doi: 10.1111/jpi.12137.
14. Fame RM, Cortés-Campos C, Sive HL. Brain Ventricular System and Cerebrospinal Fluid Development and Function: Light at the End of the Tube: A Primer with Latest Insights. *Bioessays.* 2020;42(3):e1900186. doi: 10.1002/bies.201900186.
15. Bilgiç B, Kocaman G, Arslan AB, et al. Volumetric differences suggest involvement of cerebellum and brainstem in chronic migraine. *Cephalalgia.* 2016;36(4):301-308. doi: 10.1177/0333102415588328.
16. Ducros A, Biousse V. Headache arising from idiopathic changes in CSF pressure. *Lancet Neurol.* 2015;14(6):655-668. doi: 10.1016/S1474-4422(15)00015-0.
17. Gregory K, Warner T, Cardona JJ, et al. Innervation of pineal gland by the nervus conarii: a review of this almost forgotten structure. *Anat Cell Biol.* 2023;56(3):304-307. doi: 10.5115/acb.23.037.
18. Tan DX, Manchester LC, Reiter RJ. CSF generation by pineal gland results in a robust melatonin circadian rhythm in the third ventricle as an unique light/dark signal. *Med Hypotheses.* 2016;86:3-9. doi: 10.1016/j.mehy.2015.11.018.
19. Peres MF, Masruha MR, Zukerman E, Moreira-Filho CA, Cavalheiro EA. Potential therapeutic use of melatonin in migraine and other headache disorders. *Expert Opin Investig Drugs.* 2006;15(4):367-375. doi: 10.1517/13543784.15.4.367.
20. Klein DC. Evolution of the vertebrate pineal gland: the AANAT hypothesis. *Chronobiol Int.* 2006;23(1-2):5-20. doi: 10.1080/07420520500545839.
21. Tanuri FC, de Lima E, Peres MF, et al. Melatonin treatment decreases c-fos expression in a headache model induced by capsaicin. *J Headache Pain.* 2009;10(2):105-110. doi: 10.1007/s10194-009-0097-3.
22. Ansari M, Karkhaneh A, Kheirollahi A, Emamgholipour S, Rafiee MH. The effect of melatonin on gene expression of calcitonin gene-related peptide and some proinflammatory mediators in patients with pure menstrual migraine. *Acta Neurol Belg.* 2017;117(3):677-685. doi: 10.1007/s13760-017-0803-x.
23. Lin JJ, Lin Y, Zhao TZ, et al. Melatonin Suppresses Neuropathic Pain via MT2-Dependent and -Independent Pathways in Dorsal Root Ganglia Neurons of Mice. *Theranostics.* 2017;7(7):2015-2032. doi: 10.7150/thno.19500.
24. Takahashi T, Sasabayashi D, Yücel M, et al. Pineal Gland Volume in Major Depressive and Bipolar Disorders. *Front Psychiatry.* 2020;11:450. doi: 10.3389/fpsyt.2020.00450.
25. Çiçek F, Uçar İ, Seber T, Ülkü Demir FG, Çiftçi AT. Investigation of the relationship of sleep disorder occurring in fibromyalgia with central nervous system and pineal gland volume. *Acta Neuropsychiatr.* doi: 10.1017/neu.2024.49.
26. Karabaş Ç, Karahan S, Çalış HT, Koç A. Comparison of pineal gland volume between patients with fibromyalgia and healthy controls running title: Pgv in fibromyalgia. *Eur J Ther.* 2022;28(4):301–305. doi: 10.58600/eurjther-28-4-0104.
27. Chen XY, Chen ZY, Dong Z, Liu MQ, Yu SY. Regional volume changes of the brain in migraine chronification. *Neural Regen Res.* 2020;15(9):1701-1708. doi: 10.4103/1673-5374.276360.
28. Peres MF, Valença MM, Amaral FG, Cipolla-Neto J. Current understanding of pineal gland structure and function in headache. *Cephalalgia.* 2019;39(13):1700-1709. doi: 10.1177/0333102419868187.
29. Strassman AM, Levy D. Response properties of dural nociceptors in relation to headache. *J Neurophysiol.* 2006;95(3):1298-1306. doi: 10.1152/jn.01293.2005.
30. Levy D, Labastida-Ramirez A, MaassenVanDenBrink A. Current understanding of meningeal and cerebral vascular function underlying migraine headache. *Cephalalgia.* 2019;39(13):1606-1622. doi: 10.1177/0333102418771350.
31. Zhao J, Levy D. Dissociation between CSD-Evoked Metabolic Perturbations and Meningeal Afferent Activation and Sensitization: Implications for Mechanisms of Migraine Headache Onset. *J Neurosci.* 2018;38(22):5053-5066. doi: 10.1523/JNEUROSCI.0115-18.2018.
32. Witten A, Marotta D, Cohen-Gadol A. Developmental innervation of cranial dura mater and migraine headache: A narrative literature review. *Headache.* 2021;61(4):569-575. doi: 10.1111/head.14102.
33. Li Z, Mei Y, Wang L, et al. White matter and cortical gray matter microstructural alterations in migraine: a NODDI and DTI analysis. *J Headache Pain.* 2025;26(1):115. doi: 10.1186/s10194-025-02059-3.
34. Masson R, Demarquay G, Meunier D, et al. Is Migraine Associated to Brain Anatomical Alterations? New Data and Coordinate-Based Meta-analysis. *Brain Topogr.* 2021;34(3):384-401. doi: 10.1007/s10548-021-00824-6.

https://doi.org/10.5455/annalsmedres.2025.08.230

Ann Med Res

Current issue list available at Ann Med Res

Annals of Medical Research

journal page: annalsmedres.org

Hyperbaric oxygen therapy and contralateral ear hearing thresholds in unilateral sudden sensorineural hearing loss

Taylan Zaman [a,*], Recep Ozkan [b], Kubra Ozgok Kangal [a], Osman Turkmen [c], Levent Yucel [d]

[a] University of Health Sciences, Gulhane Training and Research Hospital, Department of Undersea and Hyperbaric Medicine, Ankara, Türkiye
[b] University of Health Sciences, Van Training and Research Hospital, Department of Undersea and Hyperbaric Medicine, Van, Türkiye
[c] Samsun Training and Research Hospital, Department of Undersea and Hyperbaric Medicine, Samsun, Türkiye
[d] University of Health Sciences, Gülhane Training and Research Hospital, Department of Otorhinolaryngology, Ankara, Türkiye
*Corresponding author: taylanzaman@gmail.com (Taylan Zaman)

MAIN POINTS

- Hyperbaric oxygen therapy (HBOT) is widely used as an adjunctive treatment for idiopathic sudden sensorineural hearing loss (SSNHL) and is generally considered safe.
- This study uniquely evaluated the contralateral, clinically unaffected ears of 101 SSNHL patients undergoing HBOT.
- Hearing thresholds remained stable across 250 Hz–8 kHz, supporting the otologic safety of HBOT.
- A subtle but significant deterioration at 6 kHz (+1.98 dB, p = 0.0049) suggests chamber noise as a possible contributor.
- Findings highlight the need for high-frequency monitoring and noise-control measures in HBOT practice.

Cite this article as: Zaman T, Ozkan R, Ozgok Kangal K, Turkmen O, Yucel L. Hyperbaric oxygen therapy and contralateral ear hearing thresholds in unilateral sudden sensorineural hearing loss. *Ann Med Res*. 2026;33(2):73–78. doi: 10.5455/annalsmedres.2025.08.241.

ABSTRACT

Aim: To evaluate changes in hearing thresholds of the clinically unaffected contralateral ear before and after hyperbaric oxygen therapy (HBOT) in patients treated for unilateral idiopathic sudden sensorineural hearing loss (ISSNHL).

Materials and Methods: In this single-center retrospective observational study, pure-tone audiograms (250 Hz–8 kHz) of the contralateral ears of 101 patients who underwent HBOT were compared before and after treatment. Each session lasted approximately 120 minutes at 2.4 ATA, including compression, oxygen exposure, and decompression phases. Thresholds were age-corrected according to ISO 7029:2017. Depending on distributional assumptions, Wilcoxon signed-rank test were used for paired comparisons (α=0.05). The median number of sessions was 20 (IQR: 10–20).

Results: No significant changes were observed across most frequencies. Only at 6000 Hz, a minimal but statistically significant difference was detected (p=0.0049). The hearing thresholds at other frequencies remained stable.

Conclusion: Overall, HBOT was not associated with substantial changes in contralateral hearing thresholds. The minor threshold shift observed at 6 kHz may suggest noise exposure during treatment sessions rather than oxidative stress. This highlights the importance of monitoring high-frequency hearing and emphasizes the need for noise control measures during therapy. These findings confirm that HBOT is generally safe for the unaffected ear.

Keywords: Hyperbaric oxygen treatment, Sensorineural hearing loss, Occupational noise, Alternative therapies

Received: Aug 27, 2025 **Accepted:** Nov 13, 2025 **Available Online:** Feb 25, 2026

INTRODUCTION

Sudden sensorineural hearing loss (SSNHL) is an acute-onset condition, typically unilateral, defined as a hearing loss of ≥30 dB affecting at least three consecutive frequencies within a 72-hour window [1]. Although its etiology remains predominantly idiopathic, proposed mechanisms include viral infections, vascular compromise, autoimmune responses, and membrane ruptures. Given the risk of permanent auditory deficit, SSNHL necessitates prompt diagnosis and intervention [2].

Hyperbaric oxygen therapy (HBOT) has emerged as a critical adjunctive treatment for SSNHL. It functions by increasing arterial partial oxygen pressure, thereby facilitating oxygen diffusion to the cochlea and mitigating hypoxic injury. Cochlear hair cells—particularly the outer hair cells—are highly sensitive to oxidative stress, mechanical trauma, barometric fluctuations, and ototoxic agents [3-5]. Because these cells lack regenerative capacity in the mammalian cochlea, any significant damage typically results in permanent hearing loss.

Significant physiological effects on various organ systems, in-

cluding the auditory system, can be induced by changes in ambient pressure, whether at high altitudes or under hyperbaric conditions [6,7]. During HBOT, elevated ambient pressure and increased oxygen partial pressure may alter gas exchange, blood flow distribution, and cochlear microcirculation. Beyond pressure fluctuations, hyperbaric chambers are also significant sources of mechanical noise. A multicenter study conducted in Türkiye reported that noise levels within HBOT chambers can occasionally exceed international safety standards, particularly during the ventilation phase at treatment pressure [8]. Cochlea's dual sensitivity to pressure changes and acoustic stress highlights the need for a rigorous evaluation of the hyperbaric environment's impact on the auditory system [9].

The generation of reactive oxygen species (ROS), oxidative stress, and mitochondrial dysfunction are central to the pathophysiology of cochlear injury [4,5]. Noise exposure further exacerbates ROS production in cochlear cells, triggering DNA damage, lipid peroxidation, and apoptotic pathways. When combined with the disruption of mitochondrial membrane potential and reduced energy production, these factors can culminate in permanent sensorineural hearing loss. Consequently, strategies to prevent noise-induced hearing loss—such as reducing exposure time, utilizing protective devices, and implementing pharmacological interventions targeting oxidative stress—are essential [10]. Hyperbaric environments, where multiple stressors like pressure and noise coexist, must be managed with robust protective and monitoring protocols.

The aim of this study is to evaluate whether the noise and pressure fluctuations inherent in the hyperbaric environment induce auditory changes in the contralateral ear—which is considered clinically unaffected—in patients undergoing HBOT for unilateral SSNHL. By comparing pre- and post-treatment audiometric data, this study seeks to determine the risk of functional impairment in the healthy ear, thereby providing evidence to optimize the safety and efficacy of clinical HBOT protocols.

MATERIALS AND METHODS

Study design and participants

This retrospective cohort study was conducted at the Department of Underwater and Hyperbaric Medicine in University of Health Sciences Gülhane Training and Research Hospital. Medical records of patients who underwent HBOT for unilateral idiopathic SSNHL between February 1, 2017 and February 1, 2022 were reviewed.

Inclusion criteria were as follows: (1) diagnosis of unilateral SSNHL confirmed by pure-tone audiometry, (2) receipt of at least five HBOT sessions, and (3) availability of both baseline and post-treatment audiometric data for the contralateral (clinically unaffected) ear. Exclusion criteria included bilateral hearing loss, a history of chronic otologic disease, previous ear surgery, recent acoustic trauma, use of known ototoxic drugs within the past three months, and incomplete medical records.

Each HBOT session was conducted at 2.4 ATA for a total duration of 120 minutes, partitioned into 15 minutes of compression, 90 minutes of oxygen inhalation, and 15 minutes of decompression.

Audiological assessment

Pure-tone air-conduction thresholds dB (A) at 250 Hz, 500 Hz, 1 kHz, 2 kHz, 4 kHz, 6 kHz, and 8 kHz were measured for both ears in a soundproof booth using supra-aural headphones, in accordance with ISO 8253-1:2010. Audiometric evaluations were performed before hyperbaric oxygen therapy (pre-HBOT, baseline) and after treatment (post-HBOT, follow-up).

To control for the confounding effects of age-related hearing loss (presbycusis), thresholds were adjusted according to ISO 7029:2017 standard reference equations. These equations estimate median hearing thresholds for otologically normal individuals based on age and sex, utilizing the 18-year-old median as the 0 dB reference point [11]. For each frequency, the age-adjusted value was calculated by subtracting the predicted median threshold from the observed measured threshold.

The expected (age-adjusted) thresholds were then used to calculate correction values as follows:

ΔPre=Pre-HBOT – Expected

ΔPost=Post-HBOT – Expected

Change = ΔPost - ΔPre

Here, pre-HBOT and post-HBOT represent the hearing thresholds measured before and after treatment, respectively. In this way, the ISO 7029-adjusted hearing change for each patient was determined.

Reference noise level data

The noise data used in this study were obtained from measurements previously performed by our research team in the same multiplace hyperbaric chamber evaluated in the present study [8]. These measurements were carried out using a Brüel & Kjær Sound Level Meter Type 2240 and a Type 4231 Sound Level Calibrator under identical chamber conditions and operational protocols. Measurements were taken at a height of 130 cm above the floor and at least 1 m away from the chamber walls, corresponding to the ear level of a seated patient. The mean noise levels were 78.7 dB during compression, 84.2 dB during treatment with ventilation open, 76.0 dB with ventilation closed, and 79.1 dB during decompression. These values were used for the contextual analysis of potential noise exposure during HBOT in the present study. Although the data were cited from our previous publication, they represent the same environment and equipment used in this study.

https://doi.org/10.5455/annalsmedres.2025.08.241

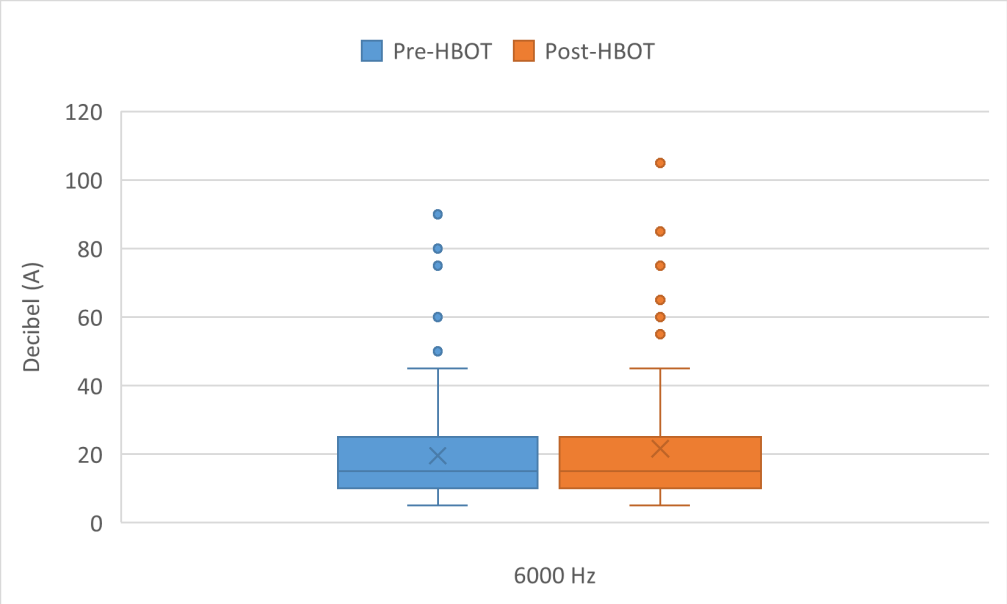

Figure 1. Change in 6 kHz pure-tone thresholds of the unaffected ear before and after HBOT.

Statistical analysis

All statistical analyses were performed using JAMOVI software, version 2.3.28 (The JAMOVI Project, Sydney, Australia). Descriptive statistics were presented as mean ± standard deviation (SD) for normally distributed variables, and as median (interquartile range, IQR) for non-normally distributed variables. Normal distribution of continuous variables was assessed by Kolmogorov–Smirnov test. The difference between present audiogram (baseline and follow-up) and age-adjusted ISO 7029:2017 standards were calculated. These differences were used in statistical analyses. The Wilcoxon signed rank test was used for analyzing the change before HBOT and after HBOT. A p-value <0.05 was considered statistically significant.

A post-hoc power analysis was conducted after study completion, based on a total sample size of N=101, an effect size of d=0.5, and a significance level of p=0.05. The analysis demonstrated a statistical power of 0.99.

Table 1. Demographic characteristics and laterality of the unaffected ear in patients with unilateral idiopathic sudden sensorineural hearing loss (ISSNHL).

Characteristic	n (%) or Median [IQR]
Sex	
Male	58 (57.4)
Female	43 (42.6)
Age (years)	42 [29--51]
Side of unaffected ear	
Right	54 (53.5)
Left	47 (46.5)
HBOT sessions	20 [10-20]

Note: Age is presented as median [Interquartile Range (IQR)]. Categorical variables are presented as absolute numbers and percentages.

RESULTS

A total of 101 patients diagnosed with unilateral idiopathic SSNHL who met the inclusion criteria were included in the analysis. The cohort consisted of 58 (57.4%) males and 43 42.6%) females, with a median age of 42 years (IQR: 29–51). The unaffected ear was the right ear in 54 patients (53.5%) and the left ear in 47 patients (46.5%). The median number of HBOT sessions completed was 20 (IQR: 10–20) (Table 1).

The pure-tone thresholds of the unaffected ear before and after HBOT, alongside the ISO 7029:2017 age-adjusted reference values, are detailed in Table 2. Across the majority of the tested frequencies (250Hz-8 kHz), both pre- and post-treatment median thresholds remained within the normal hearing range. The age-adjusted reference values were generally lower than the observed thresholds, suggesting the presence of subtle, subclinical variations in some individuals.

No statistically or clinically significant threshold shifts were observed in the contralateral (unaffected) ear at most tested frequencies, including 250 Hz, 500 Hz, 1 kHz, 2 kHz, 4 kHz, and 8 kHz. However, a minor but statistically significant change was detected at 6 kHz (p = 0.0049). This isolated high-frequency shift may reflect subtle exposure to hyperbaric chamber noise rather than the barometric or oxidative effects of HBOT (Figure 1, Table 2). This finding suggests a potential susceptibility of the unaffected ear to high-frequency environmental factors during HBOT sessions.

DISCUSSION

This study investigated whether HBOT in patients with unilateral idiopathic SSNHL induces measurable auditory changes in the contralateral ear considered clinically unaffected. Our analyses showed no significant post-treatment

https://doi.org/10.5455/annalsmedres.2025.08.241

Table 2. Comparison of pre- and post-HBOT pure-tone and age-adjusted thresholds in the unaffected ear.

Frequency (Hz)	Pre-HBOT Median (IQR) (dB)	Age-adjusted Pre-HBOT Median (IQR) (dB)	Post-HBOT Median (IQR) (dB)	Age-adjusted Post-HBOT Median (IQR) (dB)	Change Median (IQR) (dB)	P-value
250	15 (10-20)	10.46 (8.29-17.08)	15 (10-17.5)	12.73 (8.45-15)	0 (-5-5)	0.9921
500	10 (10-15)	8.54 (4.75-11.73)	10 (5-15)	6.98 (4.01-10)	0 (-5-0)	0.2426
1000	10 (5-10)	4.94 (3.71-8.16)	10 (5-10)	4.91 (3.16-9.58)	0 (0-0)	0.1729
2000	5 (5-10)	4.51 (1.76-7.77)	5 (5-10)	4.45 (1.42-5)	0 (-5-0)	0.6231
4000	10 (5-20)	4.99 (1.80-13.43)	10 (5-20)	4.81 (-0.21-13.43)	0 (-5-0)	0.1099
6000	15 (10-25)	9.27 (4.19-14.92)	15 (10-25)	9.94 (4.06-19.27)	0 (0-5)	0.0049*
8000	15 (10-25)	7.53 (2.84-12.50)	15 (10-23.75)	8.02 (0.87-15.17)	0 (0-0)	0.9483

Note: Values are expressed as median (interquartile range, 25^{th}–75^{th} percentiles). Age-adjusted medians are calculated according to ISO 7029:2017 reference equations. p-values were obtained using Wilcoxon signed-rank test due to non-normal data distribution. *$p < 0.05$ indicates statistical significance.

threshold shifts at most frequencies, although a small but statistically significant deterioration was observed at 6 kHz. The magnitude of this change was minimal; however, its statistical significance and occurrence at one of the frequencies commonly affected by noise-induced damage is noteworthy.

During HBOT, patients are exposed to increased ambient pressure and partial oxygen pressure, which may influence inner ear physiology through alterations in gas diffusion, vascular perfusion, and oxidative metabolism. HBOT is known to enhance oxygen delivery to the cochlea, thereby supporting recovery in the affected ear. However, in addition to pressure fluctuations, patients are also exposed to chamber noise generated by mechanical systems, ventilation cycles, and gas flow adjustments. A multicenter study from Türkiye reported that chamber noise levels at treatment pressure varied between 100.4 and 40.5 dB(A), reaching particularly higher values during ventilation [8]. In our clinic, noise levels during treatment depth were observed to range between 76–84.2 dB(A), and during decompression, brief peaks up to 92.3 dB(A) were recorded. Although these levels remain below most occupational exposure limits, repeated exposure across multiple sessions may exert subtle auditory effects, particularly in vulnerable frequency regions.

In noise-induced hearing loss (NIHL), the earliest audiometric finding is typically a notch at high frequencies, most often at 3, 4, or 6 kHz. The frequency at which this notch first appears varies among individuals. Initially confined to a single frequency, the notch gradually spreads to adjacent frequencies with continued noise exposure [12-14]. This vulnerability results from the combined influence of external ear canal resonance, middle ear transmission characteristics, and the tonotopic organization of the cochlea. The basal turn of the organ of Corti, which processes frequencies in the 3,000–6,000 Hz range, is particularly susceptible to mechanical and metabolic stress and thus vulnerable to injury from prolonged or intense noise exposure [12,13]. Moreover, resonance of the external auditory canal further amplifies acoustic energy in this range, increasing the risk of hair cell damage. The finding of a significant change exclusively at 6 kHz in our cohort suggests that chamber noise exposure during HBOT may produce subtle but measurable effects at higher frequencies.

The relationship between HBOT and oxidative stress is dual: while hyperoxia can transiently increase ROS production, repeated sessions may induce antioxidant responses and mitochondrial adaptation, thereby counterbalancing the net effect [15,16]. Improved cochlear oxygenation, enhanced microcirculation, and suppression of inflammation are among the proposed mechanisms underlying HBOT's therapeutic benefits [17,18]. In our cohort, the only significant difference was detected at 6 kHz, where the median change in age-adjusted threshold was 0 dB (IQR 0–5 dB), although the mean increased slightly from 19.65 dB pre-HBOT to 21.63 dB post-HBOT (Δ = +1.98 dB; $p = 0.0049$). Although this difference reached statistical significance, both the median and mean shifts remained within the clinically negligible range, indicating that no meaningful alteration in hearing function occurred. Thus, this minimal shift should be interpreted as subclinical rather than indicative of noise-induced hearing loss. We believe this minor change is more consistent with potential chamber noise exposure during treatment rather than attributable to oxidative stress itself. HBOT is generally regarded as a safe therapy; the most frequent adverse event is middle ear barotrauma, while serious complications remain rare [19,20]. Monitoring of high frequencies during treatment and implementation of in-session noise control are therefore advisable.

There are few studies evaluating contralateral ear changes in SSNHL patients undergoing HBOT. Most of the available literature has focused on functional recovery in the affected ear, while potential auditory effects on the unaffected ear have largely been overlooked. Our findings are consistent with previous studies reporting that HBOT is overall safe from an otologic standpoint. The small but statistically significant change observed at 6 kHz, although clinically minimal, aligns with known NIHL patterns and underscores the importance of monitoring the contralateral ear in HBOT protocols. Engineering measures—such as optimization of ventilation systems, maintenance of silencers, and regulation of gas flow rates—may help reduce acoustic exposure during HBOT.

The retrospective, single-center design of this study limits causal inference and generalizability. Another limitation of

https://doi.org/10.5455/annalsmedres.2025.08.241

this study is that direct in-chamber noise measurements were not performed during the HBOT sessions. Although previously collected reference data from the same HBOT unit were used, the lack of real-time measurements may limit the precision of the noise exposure assessment. The relatively short follow-up period also precluded assessment of possible delayed auditory effects. Future prospective studies should incorporate detailed monitoring of chamber noise exposure, comprehensive auditory testing, and long-term follow-up.

CONCLUSION

In this study, no changes were detected in most frequencies between 250 Hz and 8 kHz. A minimal but statistically significant difference was found at 6000 Hz ($p = 0.0049$), with no clinically relevant shift in median values. These findings suggest that HBOT is not associated with significant auditory deterioration in the unaffected ear, and that the small-scale change observed at 6000 Hz may be attributable to noise exposure during treatment sessions. While HBOT remains a generally safe adjunctive therapy, attention should be paid to noise control during treatment and to the possibility that high frequencies may be affected by noise. Prospective multicenter studies incorporating in-session noise measurements are needed to confirm these observations and to clarify the clinical significance of potential threshold shifts.

Ethics Committee Approval: This study was approved by the Ethics Committee of the University of Health Sciences Gülhane Training and Research Hospital (protocol/decision no: 2023-286, date: 22.08.2023) and was conducted in accordance with the principles of the Declaration of Helsinki.

Informed Consent: The study was retrospective, informed consent was not required from the patient.

Peer-review: Externally peer-reviewed.

Conflict of Interest: The authors declare no conflicts of interest.

Author Contributions: TZ: Conceptualization, Investigation, Methodology, Supervision, Visualization, Writing – original draft, Writing – review & editing; RO: Data curation, Investigation, Writing – review & editing; KOK: Conceptualization, Formal analysis, Methodology, Supervision, Writing – review & editing; OT: Data curation, Investigation, Writing – original draft; LY: Supervision, Writing – review & editing.

Financial Disclosure: This research did not receive any specific grant from funding agencies in the public, commercial, or not-for-profit sectors.

Artificial Intelligence Disclosure: We would like to clarify that an artificial intelligence–based tool ChatGPT (OpenAI, GPT-5.2 version) was used solely for language editing purposes, specifically to improve the clarity, grammar, and readability of the manuscript text. The AI tool was not used for study design, data analysis, data interpretation, generation of scientific content, or formulation of conclusions. All scientific content, interpretations, and conclusions are entirely the work and responsibility of the authors. The entire manuscript, including the AI-assisted language edits, was carefully reviewed, verified, and approved by the authors to ensure accuracy, originality, and scholarly integrity. The authors fully comply with the journal's ethical guidelines and confirm that no AI system is listed as an author or has any responsibility for the content of the manuscript.

REFERENCES

1. Skarżyński PH, Kołodziejak A, Gos E, Skarżyńska MB, Czajka N, Skarżyński H. Hyperbaric oxygen therapy as an adjunct to corticosteroid treatment in sudden sensorineural hearing loss: a retrospective study. *Front Neurol.* 2023;14:1225135. doi: 10.3389/fneur.2023.1225135.
2. Hua JC, Xu X, Xu ZG, et al. Aberrant Functional Network of Small-World in Sudden Sensorineural Hearing Loss With Tinnitus. *Front Neurosci.* 2022;16:898902. doi: 10.3389/fnins.2022.898902.
3. Domenico MD, Ricciardi C, Martone T, et al. Towards gene therapy for deafness. *J Cell Physiol.* 2011;226(10):2494-9. doi: 10.1002/jcp.22617.
4. Kamogashira T, Fujimoto C, Yamasoba T. Reactive Oxygen Species, Apoptosis, and Mitochondrial Dysfunction in Hearing Loss. *Biomed Res Int.* 2015;2015:617207. doi: 10.1155/2015/617207.
5. Zhang L, Du Z, He L, Liang W, Liu K, Gong S. ROS-Induced Oxidative Damage and Mitochondrial Dysfunction Mediated by Inhibition of SIRT3 in Cultured Cochlear Cells. *Neural Plast.* 2022;2022:5567174. doi: 10.1155/2022/5567174.
6. Risdall JE, Gradwell DP. Extremes of barometric pressure. *Anaesthesia & Intensive Care Medicine.* 2011;12(11):496-500. doi: 10.1016/j.mpaic.2011.08.004.
7. Jafari Z, Copps T, Hole G, Nyatepe-Coo F, Kolb B, Mohajerani MH. Tinnitus, sound intolerance, and mental health: the role of long-term occupational noise exposure. *Eur Arch Otorhinolaryngol.* 2022;279(11):5161-5170. doi: 10.1007/s00405-022-07362-2.
8. Zaman T, Celebi A, Mirasoglu B, Toklu AS. The evaluation of in-chamber sound levels during hyperbaric oxygen applications: Results of 41 centres. *Diving Hyperb Med.* 2020;50(3):244-249. doi: 10.28920/dhm50.3.244-249.
9. McKee M, James TG, Helm KVT, et al. Reframing Our Health Care System for Patients With Hearing Loss. *J Speech Lang Hear Res.* 2022;65(10):3633-45. doi: 10.1044/2022_jslhr-22-00052.
10. Harrison RV. The Prevention of Noise Induced Hearing Loss in Children. *Int J Pediatr.* 2012;2012:473541. doi: 10.1155/2012/473541.
11. International Organisation for Standardisation. Acoustics – statistical distribution of hearing thresholds related to age and gender. ISO 7029 third ed. Geneva: International Organisation for Standardisation; 2017.
12. Mirza R, Kirchner DB, Dobie RA, Crawford J; ACOEM Task Force on Occupational Hearing Loss. Occupational noise-induced hearing loss. *J Occup Environ Med.* 2018;60(9):e498-e501. doi: 10.1097/JOM.0000000000001423.
13. Lie A, Engdahl B, Hoffman HJ, Li CM, Tambs K. Occupational noise exposure, hearing loss, and notched audiograms in the HuNT Nord-Trøndelag hearing loss study, 1996-1998. *Laryngoscope.* 2017;127(6):1442-50. doi: 10.1002/lary.26256.
14. Wang Q, Qian M, Yang L, et al. Audiometric Phenotypes of Noise-Induced Hearing Loss by Data-Driven Cluster Analysis and Their Relevant Characteristics. *Front Med (Lausanne).* 2021;8:662045. doi: 10.3389/fmed.2021.662045.
15. De Wolde SD, Hulskes RH, Weenink RP, Hollmann MW, Van Hulst RA. The Effects of Hyperbaric Oxygenation on Oxidative Stress, Inflammation and Angiogenesis. *Biomolecules.* 2021;11(8):1210. doi: 10.3390/biom11081210.

https://doi.org/10.5455/annalsmedres.2025.08.241

16. Schottlender N, Gottfried I, Ashery U. Hyperbaric Oxygen Treatment: Effects on Mitochondrial Function and Oxidative Stress. *Biomolecules.* 2021;11(12):1827. doi: 10.3390/biom11121827.
17. Joshua TG, Ayub A, Wijesinghe P, Nunez DA. Hyperbaric Oxygen Therapy for Patients With Sudden Sensorineural Hearing Loss: A Systematic Review and Meta-analysis. *JAMA Otolaryngol Head Neck Surg.* 2022;148(1):5-11. doi: 10.1001/jamaoto.2021.2685.
18. Hu Y, Ye Y, Ji X, Wu J. The role of hyperbaric oxygen in idiopathic sudden sensorineural hearing loss. *Med Gas Res.* 2024;14(4):180-185. doi: 10.4103/2045-9912.385943.
19. Heyboer M 3rd, Sharma D, Santiago W, McCulloch N. Hyperbaric Oxygen Therapy: Side Effects Defined and Quantified. *Adv Wound Care (New Rochelle).* 2017;6(6):210-224. doi: 10.1089/wound.2016.0718.
20. Zhang Y, Zhou Y, Jia Y, Wang T, Meng D. Adverse effects of hyperbaric oxygen therapy: a systematic review and meta-analysis. *Front Med (Lausanne).* 2023;10:1160774. doi: 10.3389/fmed.2023.1160774.

https://doi.org/10.5455/annalsmedres.2025.08.241

Ann Med Res

Current issue list available at Ann Med Res

Annals of Medical Research

journal page: annalsmedres.org

Morton's neuroma or its mimics: Diagnostic yield of magnetic resonance imaging and radiographic markers in patients referred with a clinical suspicion

Gizem Timocin Yigman [a,*], Hande Ozen Atalay [a]

[a]*Koç University, Faculty of Medicine, Department of Radiology, Istanbul, Türkiye*
**Corresponding author: gizemtimocin1@gmail.com (Gizem Timocin Yigman)*

MAIN POINTS

- Only two-thirds of patients referred with a clinical suspicion of Morton's neuroma were confirmed to have the diagnosis on magnetic resonance imaging.
- Bursitis was the most frequent alternative diagnosis, highlighting its importance as the main differential diagnosis for MN.
- The 3/4 interphalangeal angle was significantly greater in patients with Morton's neuroma and showed diagnostic value, whereas other angular parameters were not discriminatory.
- The Vulcan sign is a specific radiographic marker for Morton neuroma but not for bursitis.
- To the best of our knowledge, this is the first study conducted exclusively in patients referred with a clinical suspicion of Morton neuroma, addressing diagnostic overlap in this unique population.

Cite this article as: Timocin Yigman G, Ozen Atalay H. Morton's neuroma or its mimics: Diagnostic yield of magnetic resonance imaging and radiographic markers in patients referred with a clinical suspicion. *Ann Med Res*. 2026;33(2):79–85. doi: 10.5455/annalsmedres.2025.09.283.

ABSTRACT

Aim: To determine the prevalence of Morton's neuroma (MN) among patients referred with a clinical suspicion of MN, identify alternative diagnoses, and assess whether angular measurements and the Vulcan sign may help differentiate.

Materials and Methods: This retrospective study included 265 feet from 244 patients (mean age, 50.7±13.0 years; 75% female) referred for magnetic resonance imaging with a presumptive diagnosis of MN between January 2020 and June 2025. All patients underwent radiography and magnetic resonance imaging. Morphometric parameters, including the hallux valgus angle, intermetatarsal angle, and interphalangeal angle (IPA), were measured according to the affected web space (2/3 or 3/4). The Vulcan sign was documented on radiographs. Statistical comparisons were performed using the Mann–Whitney U, chi-square, and Fisher's exact tests.

Results: MN was diagnosed in 167 feet (63.0%), while alternative diagnoses were in 98 (37.0%). Bursitis (32.8%), hallux valgus (30.9%), adventitial bursitis (24.5%), hallux rigidus (12.5%), and stress reaction (8.3%) were the most frequent mimics. The 3/4 IPA was significantly greater in MN than in non-MN feet ($p<0.001$).ROC analysis confirmed limited discriminatory performance, with the 3/4 IPA achieving an AUC of 0.60. Comparisons between bursitis and non-bursitis groups revealed no significant differences in any angular parameters. The Vulcan sign was significantly associated with MN in both the 2nd ($p=0.006$) and 3rd ($p<0.001$) web spaces, but no discriminatory value was found for bursitis. Its diagnostic performance was higher in the third web space (AUC 0.62) than in the second (AUC 0.51).

Conclusion: This is the first study conducted exclusively in patients referred with a clinical suspicion of MN. The 3/4 IPA demonstrated a modest yet significant association with MN, while the Vulcan sign showed relative specificity for MN compared with bursitis. These results underscore the importance of detailed assessment in clinical practice to differentiate MN from its mimics.

Keywords: Morton's neuroma, Metatarsalgia, Magnetic resonance imaging, Radiography, Diagnostic imaging, Bursitis

Received: Oct 02, 2025 **Accepted:** Dec 01, 2025 **Available Online:** Feb 25, 2026

INTRODUCTION

Metatarsalgia is defined as forefoot pain localized to the metatarsal region. A common clinical problem with a broad spectrum of potential causes. Morton's neuroma (MN) is one of the most common and well-recognized Histologically, MN does not represent a true neuroma but rather a neuro–bursal complex characterized by perineural fibrosis, axonal degeneration, and vascular proliferation [1, 2]. It typically occurs in the third intermetatarsal space, less commonly in the second, and has a marked female predominance [3, 4].

MN clinically presents with burning plantar pain, tingling or numbness of the toes, and the classic sensation of "walking on a pebble." Symptoms usually worsen with weight bearing and the use of constrictive footwear [5]. Examination find-

ings, such as Mulder's sign or palpation-induced pain in the web space, may raise suspicion, but they are not sufficiently specific to confirm the diagnosis [4]. Therefore, imaging plays a pivotal role. Ultrasound (US) is an easily accessible and dynamic modality with high sensitivity and specificity [1, 6], whereas magnetic resonance imaging (MRI) is the gold standard because of its soft tissue contrast and ability to characterize other findings [4, 7].

The differential diagnosis of MN is broad and includes intermetatarsal bursitis, plantar plate tears, metatarsophalangeal synovitis, submetatarsal bursitis (adventitious bursitis), stress fractures, tendon sheath tumors, and hallux valgus or rigidus [1, 2, 8]. These diagnoses may present similar symptoms and complicate diagnostic accuracy. In particular, intermetatarsal bursitis can easily mimic MN both clinically and radiologically and cause difficulty in accurate diagnosis [1]. In addition, forefoot static disorders, such as hallux valgus and hallux rigidus, are frequent contributors to metatarsalgia and may co-exist with MN [7, 9].

Differentiating MN from its mimics is challenging in clinical practice. Most patients referred with a preliminary diagnosis of MN have alternative pathologies, particularly bursitis [2]. Previous studies have attempted to define distinguishing imaging or clinical features to separate MN from other etiologies; however, diagnostic overlap persists [4]. Importantly, morphologic parameters have been studied in the context of forefoot disorders. To our knowledge, no previous study has specifically investigated a cohort consisting exclusively of patients referred with a clinical suspicion of MN. It is essential to systematically evaluate imaging-confirmed diagnoses and explore whether specific radiographic and MRI-based morphologic features can distinguish MN from its mimics to clarify the true prevalence of MN among such clinically suspected cases.

The aim of this study, which represents the first to focus exclusively on patients referred with a clinical suspicion of MN, is therefore to determine the proportion of patients referred with a clinical suspicion of MN who actually demonstrate MN or alternative diagnoses, to investigate whether IMA and IPA differ between patients with MN and those with other diagnoses or normal findings, and to evaluate the association between the Vulcan sign on radiographs and the presence of MN.

MATERIALS AND METHODS

This retrospective study was conducted in accordance with the principles of the Declaration of Helsinki and was approved by our institutional Biomedical Research Ethics Committee (Koç University Ethics Committee, Approval number: 2025.388.IRB2.175). All patients provided written informed consent before radiological evaluation, including permission for anonymized use of data for research purposes.

Study participants

We retrospectively reviewed patients referred with a clinical suspicion of MN who underwent both radiography and MRI of the foot between January 2020 and June 2025 at our tertiary care institution. The inclusion criterion was referral for forefoot pain with "MN?" as the clinical query. We excluded patients with prior foot surgery, known traumatic foot injuries, congenital anomalies, or examinations with nondiagnostic image quality.

Imaging protocol

All patients initially underwent radiography in standard anteroposterior and oblique projections, followed by MRI examinations using a dedicated coil and 1.5T or 3T scanners (MAGNETOM Aera and Skyra, Siemens Healthcare, Erlangen, Germany). Was examined in the supine position with the foot in neutral alignment and padded to minimize motion. Our institutional routine foot MRI protocol included coronal T1-weighted spin-echo images (TR/TE, 675/27 ms; FoV, 165×110 mm; slice thickness, 3.3 mm; acquisition matrix, 960×800); axial T1-weighted spin-echo images (TR/TE, 735/28 ms; FoV, 120×120 mm; slice thickness, 3.6 mm; acquisition matrix, 614×768); coronal proton density fat-suppressed fast spin-echo (PD-FS TSE) (TR/TE, 3250/40 ms; FoV, 165×110 mm; slice thickness, 3.0 mm; acquisition matrix, 806×768); axial PD-FS TSE (TR/TE, 4820/45 ms; FoV, 109×120 mm; slice thickness, 3.6 mm; acquisition matrix, 512×704); sagittal T1-weighted turbo inversion recovery magnitude (TIRM, fat-suppressed) images (TR/TE, 4500/28 ms; FoV, 247×180 mm; slice thickness, 3.3 mm; acquisition matrix, 352×320). Intravenous contrast was not administered in any case as per the departmental protocol for suspected MN.

Image analysis

All radiographs and magnetic resonance images were independently reviewed by two radiologists with more than 10 and 5 years of experience, respectively. MN was diagnosed when a fusiform lesion of low-to-intermediate signal on T1- and T2-weighted sequences was identified in the intermetatarsal space, typically contiguous with the plantar digital nerve. A fluid-signal lesion within the intermetatarsal bursa was defined as bursitis. Additional forefoot pathologies were systematically assessed. Hallux valgus was diagnosed on radiographs with a hallux valgus angle of >15°. Hallux rigidus was identified in the presence of joint space narrowing, osteophyte formation, and subchondral sclerosis of the first metatarsophalangeal joint and diagnosed based on both radiographs and magnetic resonance imaging. On MRI, adventitial bursitis was accepted as a fluid-signal lesion adjacent to the medial eminence of the first metatarsal head. Stress reaction was diagnosed based on marrow edema-like signal intensity on T2-weighted images without a distinct fracture line. Morphometric measurements included the HVA, IMA, and

https://doi.org/10.5455/annalsmedres.2025.09.283

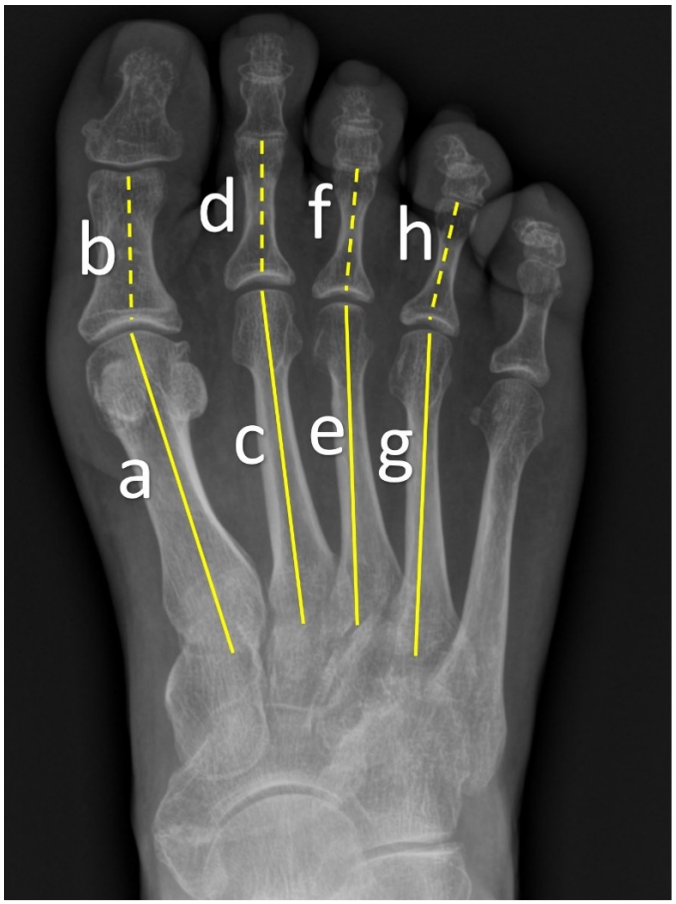

Figure 1. Measurement of angular parameters on dorsoplantar radiographs The hallux valgus angle was defined as the angle between line a (first metatarsal axis) and line b (proximal phalanx of the hallux). The 2/3 IMA was measured between lines c and e, whereas the 3/4 IMA was measured between lines e and g. The 2/3 IPA was measured between lines d and f, and the 3/4 IPA was measured between lines f and h.

IPA at the 2/3 or 3/4 interspaces depending on the pathology site. For patients with MN or bursitis in both the second and third interspaces, both corresponding angles were measured (Figure 1). On plain radiographs, the presence or absence of the Vulcan sign, which is characterized by the presence of a V-shaped appearance in the interphalangeal space, was documented at the 2/3 and 3/4 phalanx interspaces.

Statistical analysis

All statistical analyses were performed using the Statistical Package for the Social Sciences (version 28.0; IBM Corp., Armonk, NY, USA). Continuous variables, including IMA and IPA, are presented as medians with interquartile ranges. The corresponding 2/3 or 3/4 IPA and IMA were compared with those without MN in the same interspace using the Mann–Whitney U test. Separate analyses were also conducted to compare MN and bursitis cases. Patients showing both conditions in the same web space were excluded, and bursitis-positive versus bursitis-negative groups were evaluated accordingly. The presence of the Vulcan sign on radiographs was analyzed in relation to MN and bursitis within the 2nd and 3rd interspaces using Fisher's exact test or chi-square test

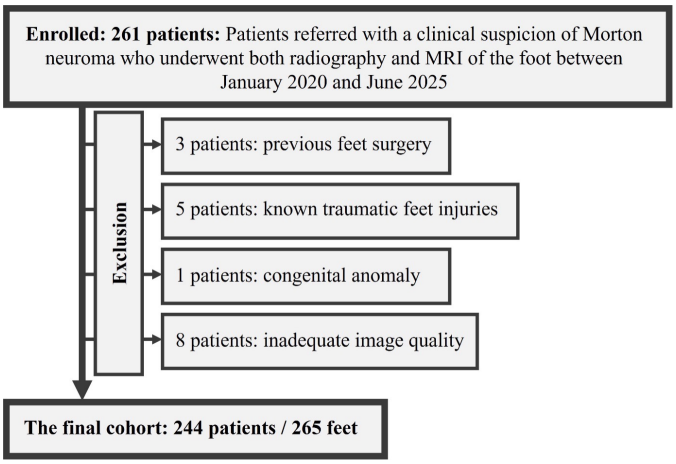

Figure 2. Flowchart of the study design.

as appropriate. In addition, ROC curve analyses were performed to assess the diagnostic performance of the 2/3 and 3/4 IPA and IMA values as well as the Vulcan sign. The area under the curve (AUC), optimal cutoff, sensitivity, and specificity were calculated for each parameter. A p-value of < 0.05 was considered statistically significant. Effect size analyses were also performed to assess the magnitude of significant associations: for Mann–Whitney U tests, the effect size ($r = Z/\sqrt{N}$) was calculated, and for categorical comparisons, Cramer's V was used. The intraclass correlation coefficient (ICC) was used to assess the interobserver reproducibility of angular measurements, and agreement for the Vulcan sign was evaluated with Cohen's kappa coefficient. A p-value of < 0.05 was considered statistically significant.

RESULTS

A total of 261 patients were initially evaluated. Of these, 3 patients were excluded due to previous foot surgery, 5 patients due to known traumatic foot injuries, and 1 patient due to congenital anomaly and 8 patients due to inadequate images for evaluation. The final cohort comprised 265 feet from 244 patients, including 21 patients with bilateral examinations (Figure 2). The mean age was 50.7±13.0 years, and 199 (75%) were female, while 66 (25%) were male.

On MRI, 167 feet (63.0%) demonstrated MN, while 98 (37.0%) did not. In our cohort, alternative diagnoses included bursitis in 87 feet (32.8%), hallux valgus in 82 (30.9%), adventitial bursitis in 65 (24.5%), hallux rigidus in 33 (12.5%), and stress reaction in 22 (8.3%) (Table 1). Multiple diagnoses were identified in 144 patients. The distribution of MN was as follows: 46 (17.4%) in web space 2, 102 (38.5%) in web space 3, and 19 (7.2%) involving both interspaces. Bursitis was observed in web space 2 in 20 cases (7.5%), in web space 3 in 24 cases (9.1%), and in both interspaces in 43 cases (16.2%). The Vulcan sign on radiographs was present in 126 patients (47.5%). Patients with MN were slightly older than those without MN (mean 52.3±12.8 vs. 48.1±13.2 years, $p<0.005$), whereas gender distribution did not differ signifi-

https://doi.org/10.5455/annalsmedres.2025.09.283

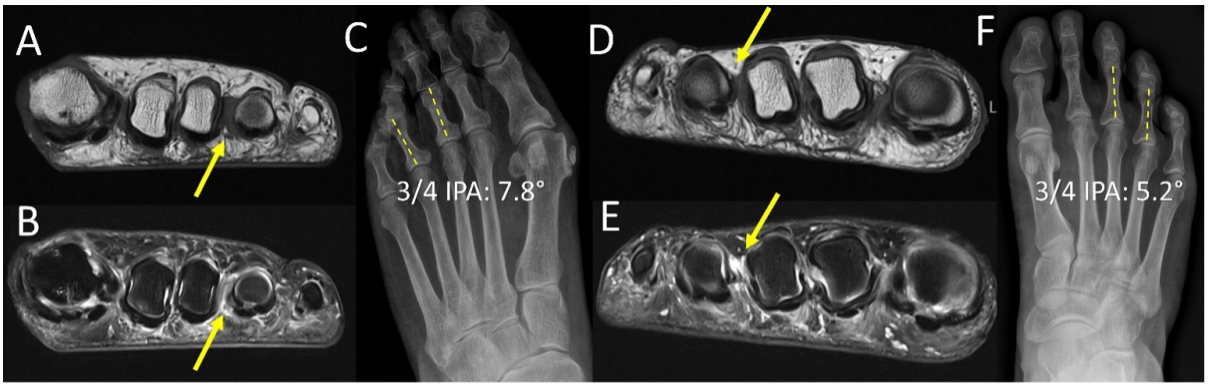

Figure 3. Comparison of the interphalangeal angle (IPA) in Morton neuroma (MN) and bursitis (A–C) A 71-year-old woman with MN in the third web space. Coronal T1-weighted (A) and fat-suppressed T2-weighted (B) magnetic resonance images show a fusiform lesion (arrows). The corresponding radiograph (C) demonstrates a 3/4 IPA of 7.8°, which is enlarged compared with non-MN cases. A 56-year-old female patient with intermetatarsal bursitis in the third web space. Coronal T1-weighted (D) and fat-suppressed T2-weighted (E) magnetic resonance images showing a fluid-signal lesion within the intermetatarsal bursa (arrows). The corresponding radiograph (F) shows a 3/4 IPA of 5.2°.

Table 1. Demographic and clinical characteristics of the study population.

Characteristic		
Total number of patients per foot		244/265
Age, mean ± SD (years)		50.7±13.0
Sex, n (%)	Female	199 (75%)
	Male	66 (25%)
Morton neuroma and its differential diagnoses	Morton neuroma, n (%)	167 (63.0%)
	Bursitis, n (%)	87 (32.8%)
	Hallux valgus, n (%)	82 (30.9%)
	Adventitial bursitis, n (%)	65 (24.5%)
	Hallux rigidus, n (%)	33 (12.5%)
	The stress reaction, n (%)	22 (8.3%)
	Multiple diagnoses (n)	144

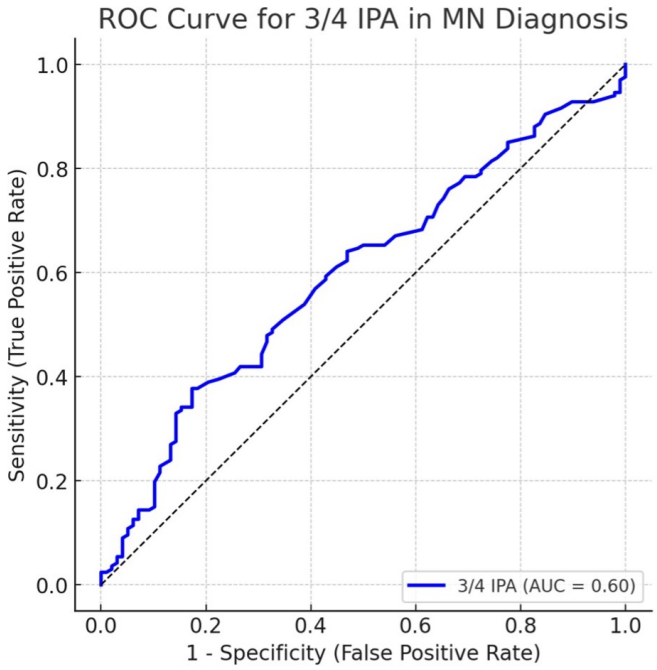

Figure 4. ROC curve of the 3/4 IPA for MN diagnosis.

Table 2. Comparison of interphalangeal angle (IPA) and intermetatarsal angle (IMA) between the Morton neuroma and non-Morton neuroma groups.

Angle	MN (median, range)	Non-MN (median, range)	p-value
2/3 IPA	4.3° (0.7–17.2)	4.2° (0.4–19.8)	= 0.96
2/3 IMA	3.2° (0.8–7.9)	3.0° (0.6–10.0)	= 0.94
3/4 IPA	5.1° (0.3–13.7)	3.6° (0.3–14.2)	< 0.001
3/4 IMA	5.2° (0.9–11.7)	4.4° (0.8–11.9)	= 0.056

IPA: interphalangeal angle; IMA: intermetatarsal angle; MN: Morton neuroma; CI, confidence interval.

Table 3. Comparison of the angles between the Bursitis and Non-Bursitis groups.

Angle	Bursitis (median, range)	Non-Bursitis (median, range)	p-value
2/3 IPA	3.4° (0.8–8.6)	4.3° (0.4–19.8)	= 0.22
2/3 IMA	2.3° (0.6–5.4)	3.1° (0.7–10.0)	= 0.056
3/4 IPA	4.0° (0.4–9.3)	4.4° (0.3–14.2)	= 0.22
3/4 IMA	5.5° (0.8–9.5)	4.5° (0.9–11.9)	= 0.27

IPA: interphalangeal angle; IMA: intermetatarsal angle.

https://doi.org/10.5455/annalsmedres.2025.09.283

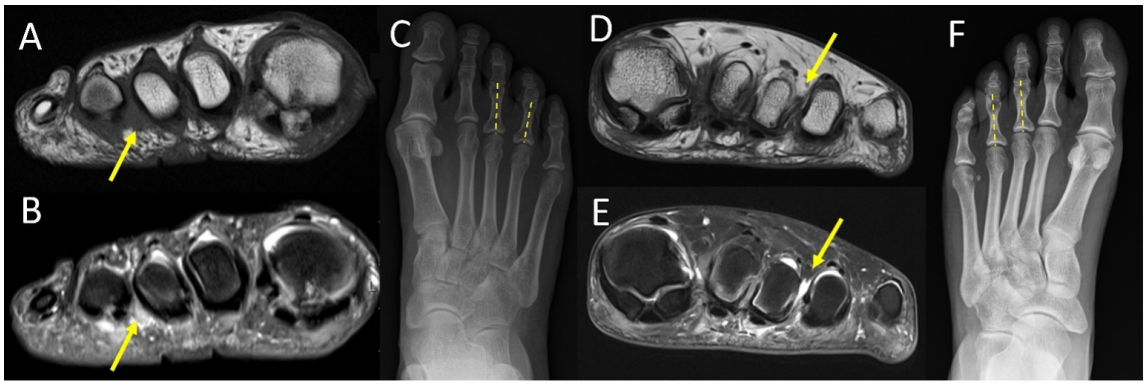

Figure 5. Comparison of the Vulcan sign in MN and bursitis. A–C. A 48-year-old woman with MN in the third web space. Coronal T1-weighted (A) and fat-suppressed T2-weighted (B) magnetic resonance images show a fusiform lesion (arrows). The corresponding radiograph (C) demonstrates a positive Vulcan sign at the 3/4 interspace. A 53-year-old female patient with intermetatarsal bursitis in the third web space. Coronal T1-weighted (D) and fat-suppressed T2-weighted (E) magnetic resonance images showing a fluid-signal lesion within the intermetatarsal bursa (arrows). The corresponding radiograph (F) shows the absence of the Vulcan sign.

Table 4. Association between the Vulcan Sign and Morton neuroma and bursitis.

Group	Web space	V-sign (+)	V-sign (--)	p-value
MN vs. Non-MN	2nd	24.6%	10.1%	= 0.006
MN vs. Non-MN	3rd	56.0%	22.3%	< 0.001
Bursitis vs. non-bursitis	2nd	10.0%	13.6%	= 1.0
Bursitis vs. non-bursitis	3rd	33.3%	40.7%	= 0.657

MN: Morton neuroma; V-sign: Vulcan sign.

Table 5. ROC analysis of interphalangeal angle and Vulcan sign.

Parameter	AUC (95% CI)	Cut-off	Sensitivity (%)	Specificity (%)
3/4 IPA	0.60 (0.53--0.66)	5.8°	37	82
V-sign (3rd web)	0.62 (0.56--0.68)	Presence	45	77
V-sign (2nd web)	0.51 (0.47--0.55)	Presence	24.6	89.9

IPA: interphalangeal angle; V-sign: Vulcan sign; AUC: Area under the curve.

cantly between the groups (p>0.005). For MN in the 2nd web space, the median 2/3 IPA was 4.3° (range, 0.7–17.2) compared with 4.2° (0.4–19.8) in non-MN feet. The corresponding IMA measured 3.2° (0.8–7.9) versus 3.0° (0.6–10.0). For MN in the third web space, the median 3/4 IPA was 5.1° (0.3–13.7) compared with 3.6° (0.3–14.2) in non-MN feet. The 3/4 IMA was 5.2° (0.9–11.7) in MN cases versus 4.4° (0.8–11.9) in non-MN cases (Table 2). For bursitis in the 2nd web space, the median 2/3 IPA was 3.4° (0.8–8.6) versus 4.3° (0.4–19.8) in non-bursitis cases, whereas the IMA was 2.3° (0.6–5.4) versus 3.1° (0.7–10.0). For bursitis in the 3rd web space, the median 3/4 IPA was 4.0° (0.4–9.3) compared with 4.4° (0.3–14.2) in non-bursitis feet, and the intermetatarsal angle was 5.5° (0.8–9.5) compared with 4.5° (0.9–11.9) (Table 3).

For MN located in the 2nd web space, neither the 2/3 IMA nor the IPA significantly differed between MN-positive and MN-negative feet (p=0.96 and p=0.94, respectively). In contrast, for MN located in the 3rd web space, the 3/4 IPA was significantly greater in MN-positive feet than in MN-negative feet (p<0.001), whereas the IMA did not differ significantly (p=0.056) (Figure 3). In addition, ROC analysis demonstrated that the 3/4 IPA achieved an AUC of 0.60 (95% CI, 0.53–0.66) with a cutoff of 5.8°, yielding 37% sensitivity and 82% specificity (Figure 4). The corresponding effect size for the 3/4 IPA was r = 0.28, indicating a small-to-moderate association between increased angle and MN.

Comparisons between bursitis and nonbursitis cases revealed no significant differences in either web space. For the 2nd web space bursitis, no significant difference was observed in both the 2/3 IPA (p=0.22) and the IMA (p=0.056) compared with the non-bursitis group, although the latter displayed a borderline trend toward higher values in bursitis cases. For the 3rd web space bursitis, neither the 3/4 IPA (p=0.22) nor the IMA (p=0.27) significantly differed between bursitis and nonbursitis feet (Figure 5).

The Vulcan sign was significantly associated with the presence of MN in the 2nd (24.6% vs. 10.1%, p=0.006) and 3rd (56.0% vs. 22.3%, p<0.001) web spaces. However, no significant association was observed between the Vulcan sign and bursitis in either the 2nd (10.0% vs. 13.6%, p=1.0) or 3rd (33.3% vs.

https://doi.org/10.5455/annalsmedres.2025.09.283

40.7%, p=0.657) web spaces (Table 4; Figure 4). In addition, the Vulcan sign achieved the highest AUC of 0.62 (95% CI 0.56–0.68), sensitivity of 45%, and specificity of 77% compared to the 2nd web space AUC of 0.51 (95% CI 0.47–0.55) (Table 5). The effect size analysis showed a small association in the 2nd web space (Cramer's V=0.17) and a moderate association in the 3rd web space (Cramer's V=0.34), supporting the stronger relationship between the Vulcan sign and MN at the 3rd interspace.

A second musculoskeletal radiologist independently repeated all angular measurements in a subset of patients to assess measurement reproducibility. The interobserver agreement was excellent, with the ICC values ranging from 0.87 to 0.94 (p<0.001). Interobserver agreement for the Vulcan sign was substantial, with $\varkappa = 0.77$ (p<0.001).

DISCUSSION

To our knowledge, this is the first study conducted in a cohort of patients referred with a clinical suspicion of MN. We demonstrated that only 63% of feet have an MN on MRI. Bursitis is the most common of the alternative diagnoses encountered, followed by hallux valgus, adventitial bursitis, hallux rigidus, and stress reaction. With respect to morphometric analyses, the 3/4 IPA was significantly greater in patients with MN than in those without, while no significant differences were observed in the 2/3 IPA or IMA measurements. In contrast, comparisons between bursitis, which is the main differential diagnosis, and non-bursitis did not yield significant differences in terms of angles. Finally, the Vulcan sign was strongly associated with MN compared with the non-MN patient group in both the 2nd and 3rd web spaces, whereas no association was observed with bursitis compared with the non-bursitis group.

Consistent with our findings, Zaleski et al evaluated 45 patients with MN and demonstrated that the 3/4 IPA was significantly increased compared with controls, with good diagnostic performance. They also reported a modest increase in the 3/4 IMA, albeit with lower specificity [10]. In contrast, we analyzed a much larger cohort of 265 feet from 244 patients in our study, and beyond confirming the diagnostic value of the 3/4 IPA, our results extend these observations by demonstrating its utility in differentiating MN from normal feet and other differential diagnoses, particularly bursitis. In contrast, two earlier studies failed to identify significant differences in IMA or IPA between MN and controls. Both studies were limited by smaller sample sizes (84 and 100 patients, respectively) and primarily focused on comparisons with controls [11, 12]. The larger sample size and unique referral-based cohort in our study likely increased the sensitivity for detecting subtle morphometric differences, particularly in the 3/4 IPA.

Galley et al evaluated 100 MN patients and 100 controls and reported that the sign had high specificity but limited sensitivity for distinguishing MN [13]. In our study, which included a larger cohort of 244 patients, a significant association was found between the Vulcan sign and MN in both the 2nd and 3rd web spaces. Importantly, we extended these observations by specifically testing its performance against bursitis, the main differential diagnosis, and demonstrated that the Vulcan sign does not discriminate between bursitis and non-bursitis cases. This consistency reinforces its role as a specific, although not sensitive, marker for MN and highlights its lack of value in separating MN from bursitis.

Finally, Togei et al approached angular measurements from a different perspective, comparing patients with and without metatarsalgia irrespective of the underlying diagnosis. They found significant differences in HVA and IMA, which were interpreted as indicators of dynamic instability rather than diagnostic indicators [14]. In contrast, our study specifically targeted a referral-based MN cohort and demonstrated the diagnostic implications of angular measurements and radiographic signs within this clinical context. From a clinical perspective, these findings suggest that simple radiographic assessment for the Vulcan sign may aid in raising suspicion for MN in patients presenting with metatarsalgia, particularly in settings where magnetic resonance imaging is not readily available. In addition, measuring the 3/4 IPA on standard imaging could provide supportive diagnostic information when interpreted alongside MRI findings, potentially improving diagnostic confidence in distinguishing MN from its mimics.

Limitations

This study has several limitations. First, the retrospective design of the study causes a potential risk of selection bias. Second, although our patient cohort is larger than those of previous studies, a larger cohort with prospective evaluation is still required. Third, clinical correlations such as pain severity, symptom duration, and functional scores were not included due to the radiological aspect of the study. Finally, although bilateral examinations were performed in 21 patients, each foot was analyzed as an independent observation because most displayed different pathologies or angular measurements between sides. Given the known asymmetry in foot morphology and deformities, such as hallux valgus, this approach was considered appropriate; however, the potential for partial interfoot dependency remains a minor limitation. In addition, although some parameters showed statistically significant associations with MN, their diagnostic performance metrics were modest, indicating limited clinical applicability when interpreted in isolation.

CONCLUSION

In conclusion, our study was conducted in the largest cohort and the first study to include patients specifically referred with a clinical suspicion of MN. It was demonstrated that nearly one-third of our cohort had alternative diagnoses rather than MN. Among the morphometric parameters, only the 3/4 IPA showed a significant association with MN at the 3rd web space,

https://doi.org/10.5455/annalsmedres.2025.09.283

whereas bursitis or other diagnoses showed no significant relationship. The Vulcan sign has emerged as a useful radiographic marker for MN but not for bursitis. These findings highlight the importance of detailed imaging evaluation in patients with metatarsalgia due to diagnostic overlap between MN and its mimics and suggest that in routine radiological evaluation for MN, IPA measurement and Vulcan sign may be helpful for correct diagnosis.

Ethics Committee Approval: This retrospective study was conducted in accordance with the Declaration of Helsinki and approved by the Biomedical Research Ethics Committee of Koc University with a reference number of 2025.388.IRB2.175 (Date: 12.09.2025).

Informed Consent: The study had retrospective design, no additional procedures were performed. Informed consent forms are obtained from each patient before the radiological examination in our institution as a clinical routine.

Peer-review: Externally peer-reviewed.

Conflict of Interest: The authors declared no potential conflicts of interest with respect to the research, authorship, and/or publication of this article.

Author Contributions: GTY: Conceptualization; Data curation; Investigation; Methodology; Project administration; Supervision; Writing–review and editing. HOA: Methodology; Formal analysis; Writing–original draft; Software.

Financial Disclosure: The authors received no financial support for the research, authorship, and/or publication of this article.

Artificial Intelligence Disclosure: AI-assisted tool (ChatGPT-5.2) was used solely for language editing.The authors are fully responsible for the content of article.

REFERENCES

1. Son HM, Chai JW, Kim YH A problem-based approach in musculoskeletal ultrasonography: central metatarsalgia. *Ultrasonography.* 2022;41(2):225-242. doi: 10.14366/usg.21193.
2. Ganguly A, Warner J, Aniq H. Central Metatarsalgia and Walking on Pebbles: Beyond Morton Neuroma. *AJR Am J Roentgenol.* 2018;210(4):821-833. doi: 10.2214/AJR.17.18460.
3. Bencardino J, Rosenberg ZS, Beltran J, Liu X, Marty-Delfaut E. Morton's neuroma: is it always symptomatic? *AJR Am J Roentgenol.* 2000;175(3):649-653. doi: 10.2214/ajr.175.3.1750649.
4. Santiago FR, Muñoz PT, Pryest P, Martínez AM, Olleta, N.P. Role of imaging methods in diagnosis and treatment of Morton's neuroma. *World J Radiol.* 2018;10(9):91-99. doi: 10.4329/wjr.v10.i9.91.
5. Jain S, Mannan K. The diagnosis and management of Morton's neuroma: a literature review. *Foot Ankle Spec.* 2013;6(4):307-317. doi: 10.1177/1938640013493464.
6. Xu Z, Duan X, Yu X, Wang H, Dong X, Xiang Z. The accuracy of ultrasonography and magnetic resonance imaging for the diagnosis of Morton's neuroma: a systematic review. *Clin Radiol.* 2015;70(4):351-8. doi: 10.1016/j.crad.2014.10.017.
7. Palka O, Guillin R, Lecigne R, Combes D. Radiological approach to metatarsalgia in current practice: an educational review. *Insights Imaging.* 2025;16(1):94. doi: 10.1186/s13244-025-01945-3.
8. Reijnierse M, Griffith JF. High-resolution ultrasound and MRI in the evaluation of the forefoot and midfoot. *J Ultrason.* 2023;23(95):e251-e271. doi: 10.15557/jou.2023.0033.
9. Coughlin MJ, Shurnas PS. Hallux rigidus: demographics, etiology, and radiographic assessment. *Foot Ankle Int.* 2003;24(10):731-743. doi: 10.1177/107110070302401002.
10. Zaleski M, Tondelli T, Hodel S, Rigling D, Wirth S. The interphalangeal angle as a novel radiological measurement tool for Morton's neuroma - a matched case-control study. *J Foot Ankle Res.* 2021;14(1):62. doi: 10.1186/s13047-021-00502-7.
11. Park YH, Jeong SM, Choi GW, Kim HJ. The role of the width of the forefoot in the development of Morton's neuroma. *Bone Joint J.* 2017;99-B(3):365-368. doi: 10.1302/0301-620X.99B3.BJJ-2016-0661.R1.
12. Naraghi R, Bremner A, Slack-Smith L, Bryant A. Radiographic Analysis of Feet With and Without Morton's Neuroma. *Foot Ankle Int.* 2017;38(3):310-317. doi: 10.1177/1071100716674998.
13. Galley J, Sutter R, Germann C, Pfirrmann CWA. The Vulcan salute sign: a non-sensitive but specific sign for Morton's neuroma on radiographs. *Skeletal Radiol.* 2022;51(3):581-586. doi: 10.1007/s00256-021-03851-3.
14. Togei K, Shima H, Hirai Y et al. Relationship Between the Relative Length of the Second Metatarsal and Occurrence of Metatarsalgia in Patients With Hallux Valgus. *Foot Ankle Int.* 2025;46(2):217-226. doi: 10.1177/10711007241298682.

https://doi.org/10.5455/annalsmedres.2025.09.283

Ann Med Res

Current issue list available at Ann Med Res

Annals of Medical Research

journal page: annalsmedres.org

Posterior tibial slope in adults with sequelae of Osgood-Schlatter disease: An MRI study

Betul Akdal Dolek [a,*], Halil Tekdemir [a], Semra Duran [a]

[a]*Ankara Bilkent City Hospital, Clinic of Radiology, Ankara, Türkiye*
**Corresponding author: b_akdal@yahoo.com (Betul Akdal Dolek)*

MAIN POINTS

- Skeletally mature adults with Osgood–Schlatter disease (OSD) sequelae show no significant differences in medial or lateral posterior tibial slope compared with matched controls on magnetic resonance imaging.
- Contrary to adolescent studies, posterior tibial slope alterations associated with OSD do not appear to persist after skeletal maturity.
- The trivial effect sizes despite adequate statistical power suggest no clinically meaningful biomechanical alteration in adult OSD sequelae.
- These findings highlight the importance of distinguishing adolescent and adult OSD when considering knee biomechanics and anterior cruciate ligament injury risk.

Cite this article as: Akdal Dolek B, Tekdemir H, Duran S. Posterior tibial slope in adults with sequelae of Osgood-Schlatter disease: An MRI study. *Ann Med Res*. 2026;33(2):86–90. doi: 10.5455/annalsmedres.2025.09.277.

ABSTRACT

Aim: Magnetic resonance imaging (MRI) assisted evaluation of the lateral and medial posterior tibial slopes in patients with Osgood-Schlatter disease (OSD) sequelae who have reached skeletal maturity.

Materials and Methods: The study population comprised 78 adults with OSD sequelae, while the control group consisted of 78 age-, sex-, and side-matched individuals without osseous, ligamentous, or tendinous pathology. A retrospective analysis of knee MRI scans was performed. The medial and lateral posterior tibial slope (PTS) angles were calculated from the sagittal T1-weighted images.

Results: Demographic variables (age, sex, and side) were statistically similar among the two groups. The medial PTS was 4.01° (95% CI: 3.41–4.61) in the OSD group and 3.90° (95% CI: 3.33–4.47) in the control group ($p = 0.784$; Cohen's $d = 0.04$). The lateral PTS was 4.98° (95% CI: 4.46–5.51) and 4.85° (95% CI: 4.29–5.41) respectively ($p = 0.732$; Cohen's $d = 0.05$). Post-hoc power analysis indicated that, with the current sample size (n = 78 per group), the study had >80% power to detect a medium effect size (Cohen's $d = 0.50$) at $\alpha = 0.05$; however, the observed differences corresponded to trivial effect sizes.

Conclusion: Contrary to findings in adolescents, skeletally mature adults with OSD sequelae did not exhibit statistical variation in medial or lateral PTS compared to matched controls. These results imply that changes in slopes described during growth may be lost after maturity.

Keywords: Osgood-Schlatter disease, Adult, Posterior tibial slope, Magnetic resonance imaging

Received: Oct 01, 2025 **Accepted:** Dec 08, 2025 **Available Online:** Feb 25, 2026

INTRODUCTION

Repetitive loading of the tibial tuberosity from quadriceps muscle activity results in Osgood-Schlatter disease (OSD), a form of traction apophysitis. It is typified by activity-related knee pain coupled with swelling and tenderness at the tibial tubercle, and it is exclusively seen in physically active adolescents, particularly boys. The condition typically manifests between ages 8–13 in girls and 10–15 in boys, with bilateral involvement reported in roughly one-quarter of patients. When skeletal growth is complete, OSD typically goes away on its own [1–5]. Ununited ossicles are a common residual finding in adults [6,7].

The shape of the proximal tibial plateau has a significant impact on knee biomechanics, with the posterior tibial slope (PTS) being especially significant [8–10]. In imaging studies, the PTS angle is the standard parameter used to quantify this feature. According to earlier studies, adolescents with OSD frequently have steeper PTS values than their peers in good health [11,12]. There is currently a lack of data on skeletally mature adults who still have OSD-related abnormalities. The aim of this study was to evaluate medial and lateral PTS in skeletally mature adults with OSD sequelae using magnetic resonance imaging (MRI). We hypothesized that there would be no significant difference in medial and lateral PTS values

https://doi.org/10.5455/annalsmedres.2025.09.277

between adult patients with OSD sequelae and matched controls.

MATERIALS AND METHODS

This study was approved by the Non-Interventional Research Ethics Committee of Bilkent City Hospital (approval number: 2-24-414). We retrospectively analyzed knee MRI examinations performed between January and December 2022. Exclusion criteria included a history of prior knee surgery or significant trauma (with radiologic evidence of ligament, tendon, or bone injury), the presence of space-occupying lesions within the knee joint, age below 20 years, and poor-quality or motion-degraded MRI scans that precluded accurate evaluation. After the exclusion of the patients that met the exclusion criteria, 78 patients with OSD sequelae were included for analyses in our study. The control group comprised 78 age-matched patients without bone, tendon or ligament disease, as determined by an MRI scan performed for anterior knee pain.

MRI acquisition

All imaging was conducted using a specialized extremity coil on a 1.5 Tesla Optima scanner (GE Medical Systems, Milwaukee, WI, USA). The knee was kept fully extended while the patients were in a supine position for the purpose of examination. The standard knee MRI protocol encompassed sagittal T1-weighted fast spin echo sequences, axial fat-suppressed PD FSE sequences, sagittal and coronal fat-suppressed PD FSE sequences, and sagittal 3D T2-weighted Cube FSE acquisitions. Slice thickness was 4.4 mm for 2D sequences with an interslice gap of 0.5 mm, while the sagittal 3D T2-weighted Cube sequence had a slice thickness of 2.15 mm with no interslice gap.

Definition of OSD sequelae

The sequelae of OSD, defined as an enlarged bony prominence in the tibial tuberosity or non-united bony fragmentation in the patellar tendon [6]. Diagnosis was based on MRI findings, and clinical history was reviewed when available to confirm consistency with prior OSD. No radiographic criteria outside MRI were required for inclusion.

Measurement of PTS

The lateral and medial PTS angles were measured using a method previously described [13]. Lateral and medial PTS were measured on the central sagittal slice, identified at the level of the posterior cruciate ligament and intercondylar eminence. The tibial axis was defined by fitting circles to the tibial cortices, and PTS was calculated relative to a perpendicular line through this axis (Figure 1A-C). All measurements were performed independently by two radiologists: one with a 20 years of experience in musculoskeletal imaging and the other with six years of experience in radiology. Inter- and intra-observer reliability were evaluated using the intraclass correlation coefficient (ICC).

Statistical analysis

SPSS software, version 20.0 (Armonk, NY: IBM Corp.) was used to conduct statistical analyses. The homogeneity of variances was confirmed using Levene's test, and the distribution of variables was examined using the Kolmogorov–Smirnov test. Independent samples t-test for continuous data and Chi-square tests for categorical data were used to compare groups. Correlation between age and PTS values was assessed using Pearson correlation analysis, as the data demon-strated normal distribution. A post-hoc power analysis was performed to evaluate the achieved statistical power using the observed effect sizes. Inter- and intra-observer reliability were assessed using the intraclass correlation coefficient (ICC). A p-value of less than 0.05 was considered statistically significant.

RESULTS

Table 1 displays the demographic characteristics of the participants. The demographic variables were similar among the OSD sequelae and control groups, with mean age (35.94 ± 12.26 vs. 35.23 ± 10.80 years, p = 0.599), sex distribution (male/female: 69/9 in both groups, p = 1.000), and side of the knee evaluated (right/left: 32/46 in both groups, p = 1.000) being highly comparable across groups. Continuous variables showed normal distribution as illustrated in Supplementary Figure 1.

Correlation analysis between age and medial/lateral PTS values did not show any significant associations (all p>0.05). Post-hoc power analysis indicated that with the current sample size (n = 78 per group), the study had >80% power to detect a medium effect size (Cohen's d = 0.50) at $\alpha = 0.05$, whereas the observed group differences corresponded to trivial effect sizes (Cohen's d < 0.10). Medial and lateral PTS values are summarized in Table 2. The mean medial PTS was 4.01° (95% CI: 3.41–4.61) in patients with OSD sequelae and 3.90° (95% CI: 3.33–4.47) in the control group (p = 0.732; Cohen's d = 0.055, 95% CI: −0.261 to 0.371). The mean

Table 1. Demographic and clinical characteristics of participants.

Variable	OSD sequelae group (n = 78)	Control group (n = 78)	P value
Gender (male/female)	69 / 9	69 / 9	1.000
Age (years, mean ± SD)	35.94 ± 12.26	35.23 ± 10.80	0.599
Side (right/left)	32 / 46	32 / 46	1.000

OSD: Osgood-Schlatter Disease; SD: Standard deviation.

Table 2. Medial and lateral posterior tibial slope (PTS) measurements in adults with OSD sequelae versus the controls.

Variable	OSD sequelae group (n = 78) (mean; 95% CI)	Control group (n = 78) (mean; 95% CI)	P value
Medial PTS (°)	4.01 (3.41--4.61)	3.90 (3.33--4.47)	0.784
Lateral PTS (°)	4.99 (4.46--5.51)	4.85 (4.29--5.41)	0.732

OSD: Osgood-Schlatter Disease; PTS: Posterior tibial slope.

https://doi.org/10.5455/annalsmedres.2025.09.277

Figure 1. Central sagittal MR images of the knee. (A) Determination of the longitudinal tibial axis using two reference circles placed at the proximal tibial shaft (red arrowhead). (B) Measurement of the medial posterior tibial slope on the central sagittal plane of the medial tibial plateau (blue arrow). (C) Measurement of the lateral posterior tibial slope on the central sagittal plane of the lateral tibi-al plateau (yellow star).

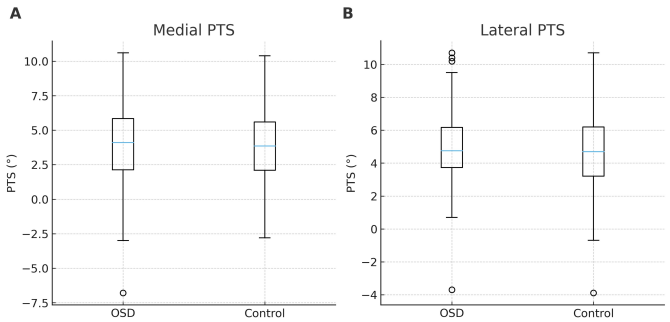

Figure 2. Boxplots depicting the distribution of medial (A) and lateral (B) posterior tibial slope values in OSD and control groups (n = 78 per group).

lateral PTS values were 4.99° (95% CI: 4.46–5.51) and 4.85° (95% CI: 4.29–5.41), respectively (p = 0.784; Cohen's d = 0.044, 95% CI: −0.272 to 0.360). Group distributions are illustrated in Figure 2.

Interobserver agreement was good to excellent, with intraclass correlation coefficients of 0.89 for medial PTS and 0.91 for lateral PTS. Intra-observer agreement was similarly excellent, with ICC values of 0.92 for medial PTS and 0.94 for lateral PTS.

Differences in medial and lateral PTS measures were statistically non-significant (p>0.05 for both). Effect size calculations confirmed the absence of clinically relevant differences, with Cohen's d values < 0.20 for both medial and lateral slopes. This suggests that, unlike in adolescents, adults with OSD sequelae do not have altered posterior tibial slope values compared to matched controls.

DISCUSSION

In this study, we investigated PTS in adults with sequelae of OSD and observed statistically non-significant differences compared with controls. Specifically, the lateral and medial PTS values were similar between the groups, suggesting that alterations in tibial plateau geometry reported in adolescents with OSD may not persist into adulthood.

OSD is among the most frequent causes of anterior knee pain in the adolescent population. It is an apophysitis of the tibial tuberosity, where the patellar tendon attaches. It is more prevalent in adolescent boys and usually resolves without treatment [1-5]. In the later stages, the detached fragment may fuse with the tibial tuberosity, giving a normal radiographic appearance, although persistent cases in adults have been described. The typical pathology of adult OSD includes an ununited ossicle and a prominent tibial tubercle [6,7]. MRI plays an important role in these cases by assessing the patellar tendon integrity, excluding other causes of anterior knee pain, and evaluating the positioning of bony fragments.

In this study, the mean age of adults with sequelae of OSD was 35 years. A rate of 88% was recorded for male patients, which was similar to the rate recorded in the Kamel et al. study [6].

In our study, the mean lateral and medial PTS values in adults with OSD sequelae were slightly higher than in the control group (4.01° vs. 3.90° and 4.99° vs. 4.85°, respectively); however, none of these differences reached statistical significance (all p>0.05). This finding indicates that, although adolescents with OSD exhibited significantly augmented PTS, these changes could diminish or become normal after skeletal maturity. Therefore, our results demonstrate that the tibial plateau morphology of adults with OSD is not different to that of adults without OSD.

The posterior tibial slope is generally defined as the angle formed between the tibial long axis and the posterior tilt of the tibial plateau [14]. Previous research has consistently shown that adolescents with OSD present with steeper PTS values than healthy counterparts. Sheppard et al. reported elevated PTS angles in both OSD patients and those with tibial tubercle fractures compared with the control group [12]. Like-

https://doi.org/10.5455/annalsmedres.2025.09.277

wise, Green et al. found significantly higher mean PTS values in adolescents with OSD (12.23° ± 3.58°) relative to controls (8.82° ± 2.76°), suggesting that asymmetric loading by the extensor mechanism during growth may contribute to this alteration [11].

Biomechanical and clinical research has emphasized that a steeper posterior tibial slope in the sagittal plane represents an important risk factor for anterior cruciate ligament (ACL) injury during childhood and adolescence [15]. In particular, an increased slope of the lateral tibial plateau has been strongly linked with a higher likelihood of ACL injury in younger patients [15].

A steeper posterior tibial slope increases anterior tibial translation and rotational stress, which may elevate the strain on the ACL. Several studies have supported this association, reporting higher ACL injury risk in patients with increased medial or lateral slope [15–18]. However, other work has shown inconsistent relationships, particularly in adults, leaving the clinical significance of PTS partially controversial [19–22]. In our study, the absence of slope differences between OSD sequelae and controls suggests that this biomechanical risk factor is unlikely to be altered in skeletally mature individuals.

In our study of skeletally mature adults with OSD sequelae, no significant differences in medial or lateral PTS were observed compared with controls. This discrepancy with adolescent studies may reflect the normalization of tibial plateau geometry following skeletal maturity. Future prospective longitudinal studies with clinical and radiologic follow-up are needed to clarify developmental changes in PTS in adults with OSD sequelae.

Although the study was adequately powered to detect medium effect sizes, the observed differences were trivial, supporting the conclusion that no clinically meaningful difference exists.

Limitations

The present study is subject to several limitations. Firstly, the retrospective design of the study, in addition to the relatively modest sample size, may reduce the generalizability of the findings. Second, only symptomatic patients were included, which may introduce selection bias. Third, data on the physical activity levels of the patients and their sports history were not available, preventing assessment of potential associations between activity and PTS measurements. Fourth, the control group consisted of patients undergoing MRI for anterior knee pain, which may not represent fully asymptomatic individuals and introduces potential selection bias.

CONCLUSION

This study found no significant difference in medial or lateral posterior tibial slope between adults with OSD sequelae and age- and sex-matched controls. The increased slope seen during growth may normalize after skeletal maturity, according to these results, which deviate from re-ports in adolescents. Clinically, this emphasizes how crucial it is to differentiate between adult and adolescent OSD when assessing the biomechanical consequences and taking the possibility of ACL damage into account.

Ethics Committee Approval: This study was approved by the Non-Interventional Research Ethics Committee of Bilkent City Hospital (2-24-414) and carried out in accordance with the Helskinki declaration of principles.

Informed Consent: Patient consent was not required because the study was retrospective.

Peer-review: Externally peer-reviewed.

Conflict of Interest: The authors declare that they have no competing interests.

Author Contributions: Conceptualization: SD, BAD; Data curation: HT Formal analysis: HT, BAD; Investigation; BAD; Methodology: SD, BAD; Project administration: BAD, SD; Resources: SD, HT; Software; HT; Supervision: SD, BAD; Validation; BAD; Visualization: BAD, SD, HT; Writing - original draft: SD, BAD; Writing - review & editing: BAD, SD.

Financial Disclosure: The research has no financial supporter.

Artificial Intelligence Disclosure: The authors declare that no artificial intelligence tools were used in the preparation of this article.

REFERENCES

1. Circi E, Atalay Y, Beyzadeoğlu T. Treatment of Osgood-Schlatter disease: Review of the literature. *Musculoskelet Surg.* 2017;101(3):195-200. doi: 10.1007/s12306-017-0479-7.
2. Neuhaus C, Appenzeller-Herzog C, Faude O. A systemic review on conservative treatment options for Osgood-Schlatter Disease. *Phys Ther Sport.* 2021;49:178-187. doi: 10.1016/j.ptsp.2021.03.002.
3. Corbi F, Matas S, Lavarez -Herms J, et al. Osgood-Schlatter Disease: Appearance, diagnosis and treatment: A narrative review. *Healthcare (Basel).* 2022;10(6):1011. doi: 10.3390/healthcare10061011.
4. Yanagisawa S, Osawa T, Takagishi K, et al. The assessment of Osgood-Schlatter disease and the skeletal maturation of the distal attachment of the patellar tendon in preadolescent males. *Orthop J Sports Med.* 2014;2(7):2325967114542084. doi: 10.1177/2325967114542084.
5. Gholve PA, Scher DM, Khakharia S, Widmann RF, Green DW. Osgood Schlatter syndrome. *Curr Opin Pediatr.* 2007;19(1):44-50. doi: 10.1097/MOP.0b013e328013dbea.
6. Kamel SI, Kanesa-Thasan R, Dave JK, et al. Prevalence of lateral patellofemoral maltracking and associated complication in patients with Osgood Schlatter disease. *Skeletal Radiol.* 2021;50(7):1399-1409. doi: 10.1007/s00256-020-03684-6.
7. Visuri T, Pihlajamäki HK, Mattila MK. Elongated patellae at the final stage of Osgood-Schlatter disease: a radiographic study. *Knee.* 2007;14(3):198-203. doi: 10.1016/j.knee.2007.03.003.
8. Chen Y, Ding J, Dai S, et al. Radiographic measurement of the posterior tibial slope in normal Chinese adults: a retrospective cohort study. *BMC Musculoskelet Disord.* 2022;23(1):386. doi: 10.1186/s12891-022-05319-4.

https://doi.org/10.5455/annalsmedres.2025.09.277

9. Bernhardson AS, DePhillipo NN, Daney BT, Kennedy MI, Aman ZS, LaPrade RF. Posterior Tibial slope and risk of posterior cruciate ligament injury. *Am J Sports Med.* 2019;47(2):312–7. doi: 10.1177/0363546518819176.
10. Chiu KY, Zhang SD, Zhang GH. Posterior slope of tibial plateau in Chinese. *J Arthroplasty.* 2000;15(2):224–7. doi: 10.1016/s0883-5403(00)90330-9.
11. Green DW, Sidharthan S, Schlichte LM, Aitchison AH, Mintz DN. Increased Posterior Tibial Slope in Patients with Osgood-Schlatter Disease: A New Association. *Am J Sports Med.* 2020;48(3):642–646. doi: 10.1177/0363546519899894.
12. Sheppard ED, Ramamurti P, Stake S, et al. Posterior Tibial Slope is Increased in Patients with Tibial Tubercle Fractures and Osgood-Schlatter Disease. *J Pediatr. Orthop.* 2021;41(6):411–416. doi: 10.1097/BPO.0000000000001818.
13. Hudek R, Schmutz S, Regenfelder F, Fuchs B, Koch P. Novel measurement technique of the tibial slope on conventional MRI. *Clin Orthop Relat Res.* 2009;467(8):2066-72. doi: 10.1007/s11999-009-0711-3.
14. Jiang J, Liu Z, Wang X, Xia Y, Wu M. Increased PTS and meniscal slope could be risk factors for meniscal injuries. A systematic review. *Arthroscopy.* 2022;38(7):2331-2341. doi: 10.1016/j.arthro.2022.01.013.
15. Edwards TC, Naqvi AZ, Cruz ND, Guptre CM. Predictors of Pediatric Anterior Cruciate Ligament Injury: The Influence of Steep Lateral Posterior Tibial Slope and Its Relationship to the Lateral Meniscus. *Arthroscopy.* 2021;37(5):1599-1609. doi: 10.1016/j.arthro.2020.12.235.
16. Oh YK, Lipps DB, Ashton-Miller JA, Wojtys EM. What strains the anterior cruciate ligament during a pivot landing? *Am J Sports Med.* 2012;40(3):574-583. doi: 10.1177/0363546511432544.
17. Zantop T, Herbort M, Raschke MJ, Fu FH, Petersen W. The role of the anteromedial and posterolateral bundles of the anterior cruciate ligament in anterior tibial translation and internal rotation. *Am J Sports Med.* 2007;35:223-227. doi: 10.1177/0363546506294571.
18. Stijak L, Herzog R, Schai P. Is there an influence of the tibial slope of the lateral condyle on the ACL lesion? A case-control study. *Knee Surg Sports Traumatol Arthrosc.* 2008;16(2):112-7. doi: 10.1007/s00167-007-0438-1.
19. Khan MS, Seon JK, Song EK. Risk factors for anterior cruciate ligament injury: assessment of tibial plateau anatomic variables on conventional MRI using a new combined method. *Int Orthop.* 2011;35(8):1251–1256. doi: 10.1007/s00264-011-1217-7.
20. Zeng C, Borim FM, Lording T. Increased posterior tibial slope is a risk factor for anterior cruciate ligament injury and graft failure after reconstruction: A systematic review. *J ISAKOS.* 2025;12:100854. doi: 10.1016/j.jisako.2025.100854.
21. Liu W, Wang B, Feng Z, Zhang H, Zhao Z, Han S. Risk-factor analysis of the proximal tibia morphology for secondary ipsilateral injury after anterior cruciate ligament reconstruction: A retrospective cross-sectional study. *Medicine (Baltimore).* 2024;103(35):e39395. doi: 10.1097/MD.0000000000039395.
22. Sorwad J, Nielsen TG, Sørensen OG, Konradsen L, Lind M. Posterior tibial slope has no impact on treatment outcome in anterior cruciate ligament revision patients. *J Exp Orthop.* 2025;12(3):e70377. doi: 10.1002/jeo2.70377.

https://doi.org/10.5455/annalsmedres.2025.09.277